Life Sciences 84 (2009) 853–856

Contents lists available at ScienceDirect

Life Sciences

journal homepage: www.elsevier.com/locate/lifescie

Involvement of asymmetric dimethylarginine (ADMA) in glomerular capillary loss and sclerosis in a rat model of chronic kidney disease (CKD)

Seiji Ueda [a,*], Sho-ichi Yamagishi [b], Yuriko Matsumoto [a], Yusuke Kaida [a], Ayako Fujimi-Hayashida [a], Kiyomi Koike [a], Hideharu Tanaka [a], Kei Fukami [a], Seiya Okuda [a]

[a] Division of Nephrology, Department of Medicine Kurume University School of Medicine, Kurume, Japan
[b] Department of Pathophysiology and Therapeutics of Diabetic Vascular Complications, Kurume University School of Medicine, Kurume, Japan

ARTICLE INFO

Article history:
Received 25 December 2008
Accepted 28 March 2009

Keywords:
ADMA
DDAH
Capillary
Endothelium
Glomerular sclerosis
Nitric oxide

ABSTRACT

Aims: Asymmetric dimethylarginine (ADMA), an endogenous nitric oxide synthase inhibitor, has been reported to be a novel marker for the progression of chronic kidney disease (CKD). We have recently found that accumulation of ADMA could trigger peritubular capillary loss, thus contributing to tubulointerstitial ischemia and fibrosis in a rat model of CKD. However, effects of ADMA on glomerular capillary loss and sclerosis remain to be elucidated.

Main methods: In this study, we investigated whether lowering of ADMA by overexpression of dimethylarginine dimethylaminohydrolase (DDAH), a main enzyme that degrades ADMA, could ameliorate glomerular capillary loss and sclerosis in a rat model of CKD. Four weeks after 5/6 subtotal nephrectomy (Nx), animals were given tail vein injections with recombinant adenovirus vector encoding DDAH-I (Adv-DDAH) or control vector expressing bacterial β-galactosidase (Adv-LZ), or orally administered with 20 mg/kg/day of hydralazine (Hyz) which served as a blood pressure control model.

Key findings: Plasma levels of ADMA were associated with decreased number of glomerular capillaries as well as severity of glomerular sclerosis in Nx-rats. These glomerular changes progressed in Adv-LZ- or Hyz-treated Nx-rats, while they were ameliorated by the treatment with DDAH overexpression.

Significance: Our present data suggest that ADMA may be involved in glomerular capillary loss and sclerosis, thus contributing to the progression of CKD. Substitution of DDAH protein or enhancement of its activity may become a novel therapeutic strategy for the treatment of CKD.

1. Introduction

Nitric oxide (NO) is synthesized by stereospecific oxidation of terminal guanidine nitrogen of L-arginine by the action of the NO synthase (NOS) (Cooke 2000; Ueda et al. 2007). The synthesis of NO can be blocked by inhibition of the NOS active site with guanidino-substituted analogues of L-arginine such as asymmetric dimethylarginine (ADMA) (Cooke 2000; Ueda et al. 2007). We, along with others, have reported that plasma levels of ADMA are elevated in patients with hypertension (Matsuoka et al. 1997; Miyazaki et al. 1999), diabetes (Miyazaki et al. 1999, Tarnow et al. 2004), and chronic kidney disease (CKD) (Vallance et al. 1992; Zoccali et al. 2001), thus suggesting that plasma ADMA level is a biomarker for future cardiovascular events in these high-risk patients (Tarnow et al. 2004; Zoccali et al. 2001; Valkonen et al. 2001; Schnabel et al. 2005).

Since several animal studies have shown that NOS inhibitors could cause systemic and glomerular hypertension, glomerular ischemia, glomerulosclerosis, tubulointerstitial injury and proteinuria (Zatz and Baylis 1998; Baylis 2008), it is conceivable that ADMA plays a role

Table 1
Clinical variables[#].

		ADMA	Ccr	UP	SBP
Adv-LZ	Before	0.71 ± 0.02	0.93 ± 0.07	7.2 ± 1.5	130 ± 7.7
	After	0.73 ± 0.02	0.77 ± ±0.09*	12.7 ± 2.7*	154 ± 15.9*
Adv-DDAH	Before	0.71 ± 0.04	1.04 ± 0.09	6.3 ± 1.2	119 ± 4.3
	After	0.55 ± 0.03*,**	1.2 ± 0.14**	7.1 ± 1.5**	122 ± 3.8**
Hydralazine	Before	0.73 ± 0.06	0.98 ± 0.19	5.2 ± 0.9	126 ± 2.2
	After	0.79 ± 0.05	0.87 ± 0.12	9.2 ± 1.6*	106 ± 10.3**

Data were expressed as mean ± S.E. Adv-LZ, Nx-rats treated with adenovirus encoding β-galactosidase; Adv-DDAH, Nx-rats treated with adenovirus encoding dimethylarginine dimethylaminohydrolase; Hydralazine, Nx-rats treated with hydralazine; ADMA, asymmetric dimethylarginine (μM); Ccr, creatinine clearance (mL/min); UP, urinary protein excretion (g/g creatinine); SBP, systolic blood pressure (mm Hg).
[#]Details or the assessment for the parameters were reported previously (Matsumoto et al. 2007).
*$P<0.05$ compared to the value of the rats before treatment.
**$P<0.05$ compared to the value of Adv-LZ.

* Corresponding author. Division of Nephrology, Department of Medicine, Kurume University, School of Medicine, 67 Asahi-machi, Kurume, 830-0011, Japan. Tel.: +81 942 31 7002; fax: +81 942 31 7763.
E-mail address: ueda@med.kurume-u.ac.jp (S. Ueda).

0024-3205/$ – see front matter © 2009 Elsevier Inc. All rights reserved.
doi:10.1016/j.lfs.2009.03.018

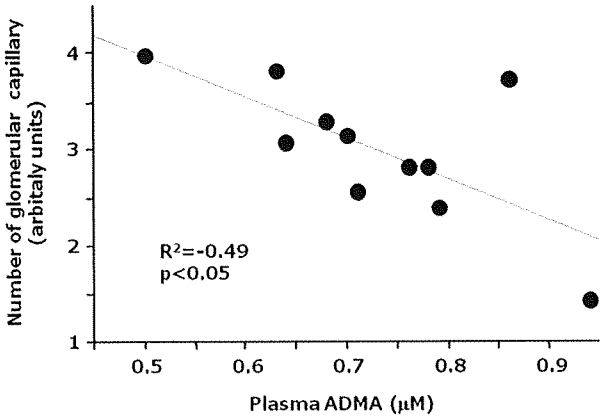

Fig. 1. A correlation between plasma levels of ADMA and number of glomerular capillaries. Four weeks after the 5/6 nephrectomy, 11 rats were killed. Then immunohistochemical analysis was performed. Glomerular capillary endothelial cells were stained with JG-12 antibody.

in the progression of CKD by inhibiting endogenous NO generation as well. Indeed, we have recently found that overexpression of dimethylarginine dimethylaminohydrolase (DDAH), a rate-limiting enzyme that degrades ADMA, blocks the elevation of blood pressure (BP) and peritubular capillary loss and subsequently reduces proteinuria in 5/6 subtotal-nephrectomized rats (Nx-rats), an experimental model of CKD by lowering ADMA levels (Matsuguma et al. 2006; Matsumoto et al. 2007). These findings have provided a basis for understanding why plasma level of ADMA could be a prognostic marker for renal impairment in patients with CKD (Fliser et al. 2005; Ravani et al. 2005). However, the pathophysiological role of ADMA on glomerular capillary loss and sclerosis remains to be elucidated. In this study, we re-analyzed the samples of our previous experiments on Nx-rats (Matsumoto et al. 2007) in order to clarify whether lowering of ADMA by overexpression of DDAH could ameliorate glomerular capillary loss and sclerosis in the rat model of CKD.

2. Materials and methods

2.1. Materials

Recombinant adenoviruses encoding human DDAH-I (Adv-DDAH), the entire coding region of DDAH and bacterial β-galactosidase (Adv-LZ) were prepared as described previously (Ueda et al. 2003).

2.2. Experimental protocol

Detail experimental procedure was described previously (Matsumoto et al. 2007). Briefly, 4 weeks after nephrectomy (Nx), the rats were randomly divided into 4 groups; rats immediately killed ($n=11$), rats treated with tail vein injection of 1.5×10^{10} plaque-forming units of Adv-DDAH ($n=15$) or control adenovirus vector expressing bacterial a-galactosidase (Adv-LZ) ($n=15$), rats orally administered with 20 mg/kg/day of hydralazine (Hyz), which served as a BP control model ($n=6$). Fourteen days after the treatment, the rats were sacrificed. All experimental procedures were conducted in accord with the NIH Guide for the Care and Use of Laboratory Animals and were approved by the ethical committee of our institution.

2.3. Chemical analysis

Plasma levels of ADMA were measured by high-performance liquid chromatography as described previously (Matsuguma et al. 2006; Matsumoto et al. 2007; Ueda et al. 2003).

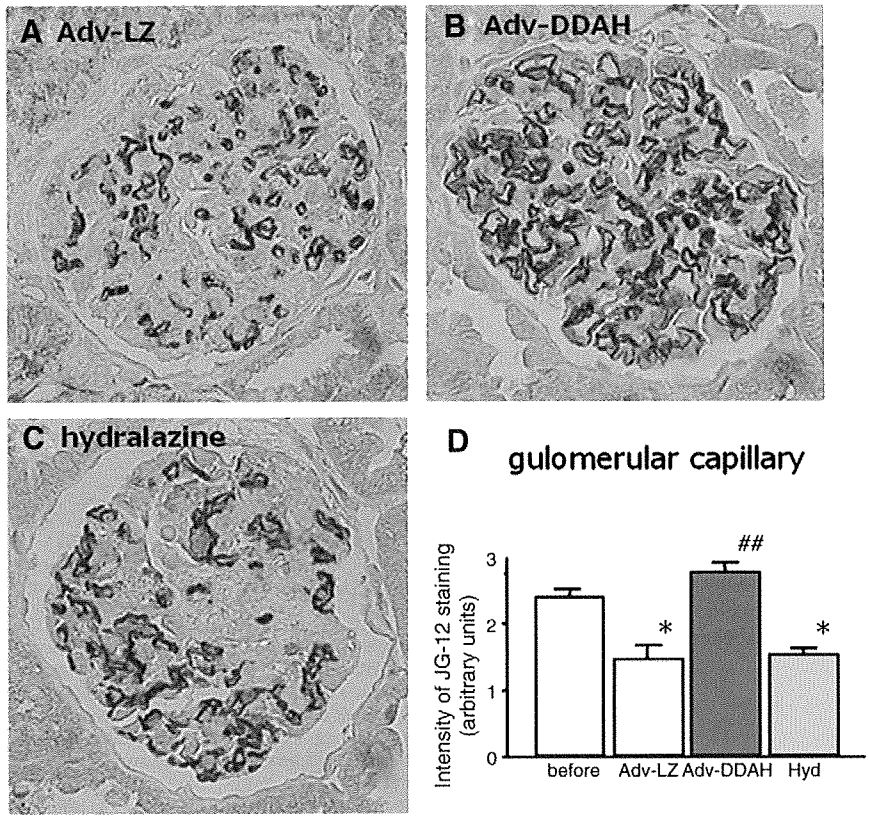

Fig. 2. Effects of DDAH overexpression on progressive loss of glomerular capillaries. Representative data of immunohistochemistry are shown. (A) Adv-LZ-treated Nx-rats. (B) Adv-DDAH-treated Nx-rats. (C) Hyz-treated Nx-rats (Hyd). (D) Quantitative analysis of immunostaining of glomerular capillaries. *$P<0.05$ compared to the value before treatment. ##$P<0.01$ compared to the value of Adv-LZ or Hyz-treated rats.

2.4. Immunohistochemistry

The kidneys were removed and fixed in 4% paraformaldehyde. Then the kidneys were embedded in paraffin wax for sectioning. Three-micrometer paraffin sections were incubated with monoclonal JG-12 antibody raised against aminopeptidase P of capillary endothelial cells (Bender MedSystems, San Bruno, CA). After exposure to peroxidase-labeled secondary anti-mouse antibody, the sections were incubated with 3,3′-diaminobenzidine solution. The intensity of JG-12 staining was analyzed by an image analysis software (Optimas version 6.57; Media Cybernetics, Silver Spring, MD).

2.5. Renal histology analysis

Three-micrometer paraffin sections were stained with periodic acid-Schiff (PAS) to evaluate glomerular sclerosis. To semi-quantitate glomerular sclerosis, 50 glomeruli were selected at random, and the degree of glomerular matrix expansion was determined as previously described (Tamaki et al. 1994). The percentage of each glomerulus occupied by a mesangial matrix was estimated and assigned a score beginning with 0 = 0%, 1+ = 1 to 25%, 2+ = 26 to 50%, 3+ = 51 to 75% and 4+ = 76 to 100%. The number of glomeruli showing a lesion of 0 was set n0, 1 + n1, 2 + n2, 3 + n3, 4 + n4, respectively. Fifty glomeruli were examined independently, and then the sclerosis index was obtained by the following formula: $(0\times n0 + 1\times n1 + 2\times n2 + 3\times n3 + 4\times n4) / 50 \times 100$.

2.6. Statistical analysis

All data were expressed as mean ± S.E. Experimental groups were compared by analysis of variance (ANOVA), and, when appropriate, with Scheffe's test for multiple comparisons. Linear regression analysis was performed between plasma ADMA and glomerular capillary density. A level of $P<0.05$ was accepted as statistically significant.

3. Results

3.1. Data of clinical variables

As previously reported (Matsumoto et al. 2007), baseline creatinine clearance (Ccr), urinary excretion of protein levels (UP), and systemic BP (SBP) were similar among three groups (Table 1). Treatment with Adv-DDAH, but not Adv-LZ or Hyz, significantly decreased plasma levels of ADMA (Table 1) and subsequently ameliorated Ccr in Nx-rats (Table 1). SBP were progressively elevated in Adv-LZ-transfected Nx-rats, whereas that of Adv-DDAH-transfected Nx-rats remained unchanged (Table 1). Hyz treatment prevented the elevation of BP levels in Nx-rats as well (Table 1).

3.2. Relationship between plasma ADMA levels and glomerular capillary loss

We first investigated the relationship between plasma ADMA levels and glomerular endothelium in Nx-rats. As shown in Fig. 1, plasma levels of ADMA were correlated with decreased number of glomerular capillaries in Nx-rats (Fig. 1).

3.3. Effects of DDAH overexpression on glomerular changes

We next investigated the effects of Adv-DDAH on glomerular changes in Nx-rats. As shown in Figs. 2 and 3, progressive loss of glomerular capillaries and accelerated glomerular sclerosis were observed in Adv-LZ- or Hyz-treated Nx-rats, which were significantly blocked by the treatment with Adv-DDAH.

4. Discussion

The salient findings of this study are (1) plasma levels of ADMA were associated with decreased number of glomerular capillaries in Nx-rats (Figs. 1 and 2) overexpression of DDAH-I, a rate-limiting enzyme that degrades ADMA, decreased plasma levels of ADMA and subsequently prevented the progressive loss of glomerular capillaries and accelerated glomerular sclerosis in Nx-rats (Figs. 2 and 3). Although Hyz treatment blocked the elevation of BP, it did not decrease plasma ADMA level or improve these glomerular changes in Nx-rats. Therefore, the present results suggest that DDAH overexpression blocks the progression of glomerular damage in a rat model of CKD by reducing plasma levels of ADMA, but not lowering BP levels.

It has been previously reported that blockade of NO generation increases systemic and glomerular pressure and subsequently causes

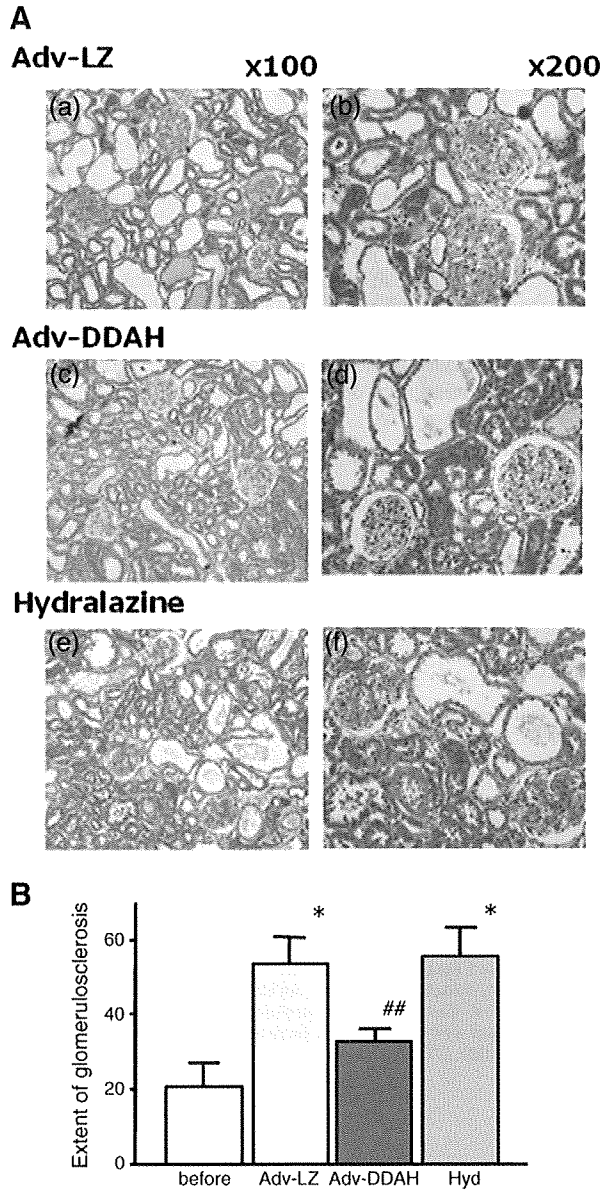

Fig. 3. Effects of DDAH overexpression on glomerular sclerosis. A. Representative data of PAS staining are shown. (a) and (b), Adv-LZ-treated Nx-rats; (c) and (d), Adv-DDAH-treated Nx-rats; (e) and (f), Hyz-treated Nx-rats. Magnification, ×100 ((a), (c), (e)). ×200 ((b), (d), (f)). B. Quantitative analysis of the extent of glomerular sclerosis. *$P<0.05$ compared to the value before treatment. ##$P<0.01$ compared to the value of Adv-LZ or Hyz-treated rats.

glomerular sclerosis in Nx-rats (Zatz and Baylis 1998; Baylis 2008; Kang et al. 2002). Further, it has been reported that glomerular endothelial cell injury or loss is observed in the early phase of renal ablation, which could lead to glomerular sclerosis in this model (Lee et al. 1995; Shimizu et al. 1997). Since NO is known as a critical factor for endothelial function and endothelial cell survival and repair (Murohara et al. 1998; Konishi et al. 2007), it is conceivable that ADMA could cause glomerular capillary damage and subsequently elicit glomerular sclerosis in Nx-rats by inhibiting endogenous NO production. In support of this, DDAH overexpression enhances VEGF expression in cultured endothelial cells and stimulates tube formation of these cells (Smith et al. 2003). In a murine model of hindlimb ischemia, enhanced neovascularization and limb perfusion are observed in DDAH transgenic mice, which are associated with reduced plasma levels of ADMA (Jacobi et al. 2005). Further, it has been reported that VEGF administration enhances glomerular capillary repair and accelerates resolution of experimentally induced glomerulonephritis (Masuda et al. 2001). We have recently found that DDAH overexpression blocks peritubular capillary loss as well as tubulointerstitial ischemia and fibrosis in the same remnant kidney model (Matsumoto et al. 2007).

5. Conclusion

In conclusion, these observations suggest that impairment of the ADMA-DDAH axis in Nx-rats, that is, decreased renal expression of DDAH and elevation of ADMA in a rat model of CKD (Matsuguma et al. 2006; Matsumoto et al. 2007), could cause glomerular and peritubular capillary loss and subsequently elicits glomerular sclerosis and tubulointerstitial fibrosis, thus leading to the progression of CKD. Substitution of DDAH protein or enhancement of its activity may become a novel therapeutic strategy for the treatment of CKD.

Acknowledgments

This work was supported in part by a grant from Grant-in-Aid for Scientific Research from the Ministry of Education, Science and Culture, Tokyo; a grant from Japan Foundation of Cardiovascular Research, Tokyo; and a grant from the Ishibashi Foundation for the Promotion of Science, Kurume, Japan.

References

Baylis C. Nitric oxide deficiency in chronic kidney disease. American Journal of Physiology. Renal Physiology 294 (1), F1–9, 2008.

Cooke JP. Dose ADMA cause endothelial dysfunction? Arteriosclerosis, Thrombosis, and Vascular Biology 20 (9), 2032–2037, 2000.

Fliser D, Kronenberg F, Kielstein JT, Morath C, Bode-Boger SM, Haller H, Ritz E. Asymmetric dimethylarginine and progression of chronic kidney disease: The mild to moderate kidney disease study. Journal of the American Society of Nephrology 16 (8), 2456–2461, 2005.

Jacobi J, Sydow K, von Degenfeld G, Zhang Y, Dayoub H, Wang B, Patterson AJ, Kimoto M, Blau HM, Cooke JP. Overexpression of dimethylarginine dimethylaminohydrolase reduces tissue asymmetric dimethylarginine levels and enhances angiogenesis. Circulation 111 (11), 1431–1438, 2005.

Kang DH, Nakagawa T, Feng L, Johnson RJ. Nitric oxide modulates vascular disease in the remnant kidney model. The American Journal of Pathology 161 (1), 239–248, 2002.

Konishi H, Sydow K, Cooke JP. Dimethylarginine dimethylaminohydrolase promotes endothelial repair after vascular injury. Journal of the American College of Cardiology 49 (10), 1099–1105, 2007.

Lee LK, Meyer TW, Pollock AS, Lovett DH. Endothelial cell injury initiates glomerular sclerosis in the rat remnant kidney. The Journal of Clinical Investigation 96 (2), 953–964, 1995.

Masuda Y, Shimizu A, Mori T, Ishiwata T, Kitamura H, Ohashi R, Ishizaki M, Asano G, Sugisaki Y, Yamanaka N. Vascular endothelial growth factor enhances glomerular capillary repair and accelerates resolution of experimentally induced glomerulonephritis. The American Journal of Pathology 159 (2), 599–608, 2001.

Matsuguma K, Ueda S, Yamagishi S, Matsumoto Y, Kaneyuki U, Shibata R, Fujimura T, Matsuoka H, Kimoto M, Kato S, Imaizumi T, Okuda S. Molecular mechanism for elevation of asymmetric dimethylarginine (ADMA) and its role for hypertension in chronic kidney disease. Journal of the American Society of Nephrology 17 (8), 2176–2183, 2006.

Matsumoto Y, Ueda S, Yamagishi S, Matsuguma K, Shibata R, Fukami K, Matsuoka H, Imaizumi T, Okuda S. Dimethylarginine dimethylaminohydrolase prevents progression of renal dysfunction by inhibiting loss of peritubular capillaries and tubulointerstitial fibrosis in a rat model of chronic kidney disease. Journal of the American Society of Nephrology 18 (5), 1525–1533, 2007.

Matsuoka H, Itoh S, Kimoto M, Kohno K, Tamai O, Wada Y, Yasukawa H, Iwami G, Okuda S, Imaizumi T. Asymmetrical dimethylarginine, an endogenous nitric oxide synthase inhibitor, in experimental hypertension. Hypertension 29 (1 Pt 2), 242–247, 1997.

Miyazaki H, Matsuoka H, Cooke JP, Usui M, Ueda S, Okuda S, Imaizumi T. Endogenous nitric oxide synthase inhibitor: A novel marker of atherosclerosis. Circulation 99 (9), 1141–1146, 1999.

Murohara T, Asahara T, Silver M, Bauters C, Masuda H, Kalka C, Kearney M, Chen D, Symes JF, Fishman MC, Huang PL, Isner JM. Nitric oxide synthase modulates angiogenesis in response to tissue ischemia. The Journal of Clinical Investigation 101 (11), 2567–2578, 1998.

Ravani P, Tripepu G, Mallberti F, Testa S, Mallamaci F, Zoccali C. Asymmetrical dimethylarginine predicts progression to dialysis and death in patients with chronic kidney disease: A competing risks modeling approach. Journal of the American Society of Nephrology 16 (8), 2449–2455, 2005.

Schnabel R, Blankenberg S, Lubos E, Lackner KJ, Rupprecht HJ, Espinola-Klein C, Jachmann N, Post F, Peetz D, Bickel C, Cambien F, Tire L, Munzel T. Asymmetric dimethylarginine and the risk of cardiovascular events and death in patients with coronary artery disease: Results from the AtheroGene Study. Circulation Research 97 (5), e53–59, 2005.

Shimizu A, Kitamura H, Masuda Y, Ishizaki M, Sugisaki Y, Yamanaka N. Rare glomerular capillary regeneration and subsequent capillary regression with endothelial cell apoptosis in progressive glomerulonephritis. The American Journal of Pathology 151 (5), 1231–1239, 1997.

Smith CL, Birdsey GM, Anthony S, Arrigoni FI, Leiper JM, Vallance P. Dimethylarginine dimethylaminohydrolase activity modulates ADMA levels, VEGF expression, and cell phenotype. Biochemical and Biophysical Research Communications 308 (4), 984–989, 2003.

Tamaki K, Okuda S, Ando T, Iwamoto T, Nakayama M, Fujishima M. TGF-beta 1 in glomerulosclerosis and interstitial fibrosis of adriamycin nephropathy. Kidney International 45 (2), 525–536, 1994.

Tarnow L, Hovind P, Teerlink T, Stehouwer CD, Parving HH. Elevated plasma asymmetric dimethylarginine as a marker of cardiovascular morbidity in early diabetic nephropathy in type 1 diabetes. Diabetes Care 27 (3), 765–769, 2004.

Ueda S, Kato S, Matsuoka H, Kimoto M, Okuda S, Morimatsu M, Imaizumi T. Regulation of cytokine-induced nitric oxide synthesis by asymmetric dimethylarginine: Role of dimethylarginine dimethylaminohydrolase. Circulation Research 92 (2), 226–233, 2003.

Ueda S, Yamagishi S, Matsumoto Y, Fukami K, Okuda S. Asymmetric dimethylarginine (ADMA) and cardiovascular disease. Clinical and Experimental Nephrology 11 (2), 115–121, 2007.

Valkonen VP, Paiva H, Salonen JT, Lakka TA, Lehtimaki T, Laakso S, Laaksonen R. Risk of acute coronary event and serum concentration of asymmetrical dimethylarginine. Lancet 358 (9299), 2127–2128, 2001.

Vallance P, Leone A, Calver A, Collier JJ, Moncada S. Accumulation of an endogenous inhibitor of nitric oxide synthesis in chronic renal failure. Lancet 339 (8793), 572–575, 1992.

Zatz R, Baylis C. Chronic nitric oxide inhibition model six years on. Hypertension 32 (6), 958–964, 1998.

Zoccali C, Bode-Böger SM, Mallamaci F, Benedetto F, Tripepi G, Malatino L, Cataliotti A, Bellanuova I, Fermo I, Frolich J, Boger RH. Plasma concentration of asymmetrical dimethylarginine and mortality in patients with end-stage renal disease: A prospective study. Lancet 358 (9299), 2113–2117, 2001.

NDT Advance Access published May 22, 2009

Nephrol Dial Transplant (2009) 1 of 9
doi: 10.1093/ndt/gfp214

Original Article

NDT
Nephrology Dialysis Transplantation

IL-1RI deficiency ameliorates early experimental renal interstitial fibrosis

Lynelle K. Jones[1], Kim M. O'Sullivan[1], Timothy Semple[1], Michael P. Kuligowski[1], Kei Fukami[2], Frank Y. Ma[3], David J. Nikolic-Paterson[1,3], Stephen R. Holdsworth[1,3] and A. Richard Kitching[1,3,4]

[1]Department of Medicine, Centre for Inflammatory Diseases, Monash University, Monash Medical Centre, Clayton, [2]Vascular Division, The Baker Heart Research Institute, Danielle Alberti Memorial Centre for Diabetes Complications, Melbourne, [3]Department of Nephrology and [4]Department of Paediatric Nephrology, Monash Medical Centre, Clayton, Victoria, Australia

Correspondence and offprint requests to: A. Richard Kitching; E-mail: richard.kitching@med.monash.edu.au

Abstract

Background. IL-1β has the potential to promote progressive renal disease by effects on macrophage recruitment and activation or by effects mediated through tubular cell transforming growth factor (TGF)-β production, previously demonstrated *in vitro*.

Methods. The *in vivo* roles of endogenous IL-1β and its type I receptor (IL-1RI) in renal fibrosis were studied using wild-type C57BL/6 mice, IL-1β$^{-/-}$ and IL-1RI$^{-/-}$ mice with unilateral ureteric obstruction.

Results. After 7 days, IL-1RI$^{-/-}$ mice (IL-1α and IL-1β deficient) were protected from injury and collagen accumulation. IL-1β$^{-/-}$ mice demonstrated some histological protection, but no reduction in α1(1) procollagen mRNA or biochemically measured collagen accumulation. Compared with obstructed kidneys from wild-type mice, TGF-β1 mRNA was reduced in IL-1RI$^{-/-}$ mice (with trends to reduced TGF-β2 and TGF-β3). Expression of a downstream TGF-β effector, connective tissue growth factor, was decreased in IL-1RI$^{-/-}$ mice. IL-1RI$^{-/-}$ mice exhibited less tubulointerstitial apoptosis compared with wild-type mice. Macrophage infiltration and adhesion molecule mRNA expression was unchanged in IL-1β$^{-/-}$ or IL-1RI$^{-/-}$ mice. While TNF expression was similar to wild-type mice, IFN-γ expression was reduced in both IL-1β$^{-/-}$ and IL-1RI$^{-/-}$ mice. IL-1RI$^{-/-}$ mice at 14 days showed a catch-up in fibrosis compared with wild-type mice.

Conclusion. IL-1/IL-1RI interactions are profibrotic in renal fibrosis. IL-1RI$^{-/-}$ mice were more protected at an early stage, associated with changes in TGF-β and downstream mediators of fibrosis, but independent of the presence of infiltrating macrophages.

Keywords: IL-1; interstitial fibrosis; macrophages; obstructive uropathy; TGF-β

Introduction

Tubulointerstitial fibrosis is a common pathway to end-stage renal failure occurring after a variety of immune and inflammatory, metabolic or haemodynamic renal insults. The initiating injury, timing and persistence of the initiating insult are all important in tubulointerstitial fibrosis. However, observations from human disease and *in vitro* and *in vivo* models have defined several processes common to tubulointerstitial fibrosis induced by a variety of different insults. These include tubular injury, the infiltration of innate immune effectors, epithelial myofibroblast transformation and the laying down of matrix proteins, including collagens and fibronectin, with resulting interstitial fibrosis, tubular atrophy and loss of renal function [1–3].

Potential pro-fibrogenic mediators present in the tubulointerstitium include cytokines, secreted by immune/inflammatory cells and/or intrinsic renal cells. IL-1β possesses a variety of proinflammatory effects relevant to a range of diseases [4,5]. IL-1β binds to the IL-1 receptor (IL-1RI), constitutively expressed at low levels on most cells, including 'immune' cells, endothelial cells, epithelial cells and fibroblasts [4]. Another member of the IL-1 family, IL-1α, can bind to and signal via this receptor. IL-1α plays an autocrine role in cell activation, being expressed on the cell surface, intracellularly and also released from cells [4,5]. The IL-1 receptor antagonist (IL-1Ra) antagonizes the activity of IL-1 *in vivo* by competitively binding to IL-1RI [6]. Another membrane receptor, IL-1RII, acts as a decoy receptor and does not signal on binding to IL-1 [7]. Both IL-1RI and IL-1RII can exist in soluble forms [4]. IL-1β has a number of biological actions that might promote fibrosis, including promoting leukocyte infiltration, inducing proinflammatory mediators and inducing the production of transforming growth factor (TGF-β), a key profibrotic growth factor. *In vitro*, both IL-1α and IL-1β promote TGF-β production [8–10] as well as fibronectin production and loss of E-cadherin expression (by IL-1α) or induction of α-smooth muscle actin (α-SMA, a

myofibroblast marker) expression (by IL-1β). These changes in primary cultures of human proximal tubular cells are TGF-β dependent [8,10]. Both IL-1α and IL-1β are produced by fibroblasts [11,12]. IL-1 has similar effects on TGF-β and matrix production in cultured cortical fibroblasts and also promotes fibroblast proliferation [11,13], and fibroblasts derived from diseased kidneys demonstrate greater IL-1 responsiveness than those from normal kidneys [11,12].

Obstructive uropathy is an important cause of renal fibrosis, with the involvement of macrophages, tubular cells and apoptosis of tubular cells, interstitial myofibroblasts, soluble cytokines/growth factors (the best known being TGF-β), proteolytic enzymes and matrix proteins [5,14–16]. It is commonly modelled by ligating one ureter (unilateral ureteric ligation, UUO) in mice. In this system, bone marrow-derived CD11b+ and CD18+ cells modified to overexpress IL-1Ra limit injury in murine UUO after 6 days [17]. The hypothesis tested by the current studies was that mice genetically deficient in IL-1β or the IL-1RI would be protected from experimental interstitial fibrosis induced by UUO.

Methods

Experimental mice

Mice with a deletion of the IL-1β (IL-1β$^{-/-}$, from Y. Iwakura, University of Tokyo, Tokyo, Japan [18]) or the IL-1R1 gene (IL-1RI$^{-/-}$, from A. Satsokar, Ohio State University, OH, USA [19]) on a C57BL/6 background were bred in an SPF facility (Monash Medical Centre, Clayton, Victoria, Australia). Male mice (6–8 weeks old) were used. The left ureter was ligated under general anaesthesia [20] and renal injury was studied after 7 or 14 days. Experiments were approved by the Monash University, Monash Medical Centre Animal Ethics Committee. Histological assessment was performed on coded slides, results expressed as mean ± SD. For analysis of two groups, the significance of differences between groups was determined by an unpaired *t*-test, and for more than two groups by ANOVA, with Tukey's post-test (Prism, GraphPad Software, San Diego, CA, USA). Seven days after UUO, C57BL/6 wild-type (WT) mice (n = 7), IL-1β$^{-/-}$ mice (n = 13) and IL-1RI$^{-/-}$ mice (n = 7) were studied. For 14-day analyses, C57BL/6 WT mice (n = 7) and IL-1RI$^{-/-}$ mice (n = 9) were studied.

Detection of IL-1RI in mice subjected to UUO

Renal IL-1RI protein was demonstrated using anti-mouse CD121a (IL-1 receptor type I/p80, 35F5, BD Biosciences, San Jose, CA, USA) conjugated with R-phycoerythrin. Cryostat-cut snap frozen sections (6 μm) were incubated with 15% rat serum in 5% BSA/PBS (10 min, room temperature) and then with anti-IL-1RI-PE (1:50 in 1% BSA/PBS; 1 h, room temperature). Sections from IL-1RI$^{-/-}$ mice were negative controls.

Assessment of morphological changes and collagen accumulation

Kidney tissues were fixed in Bouin's fixative and embedded in paraffin, and 3-μm tissue sections from all mice were stained with picrosirius red (Sigma, St Louis, MO, USA) identifying collagen fibres (red) [20,21]. Histological assessment of matrix deposition was determined by point counting using a 10 × 10 grid. A minimum of 10 high power fields (×400, hpf) were assessed per animal, and results expressed as % interstitial cortical area, excluding glomeruli, blood vessels, periglomerular and perivascular areas [20,22]. Renal collagen content was measured by determining total hydroxyproline [23] as previously described [20], and results expressed as μg/mg kidney wet weight.

Interstitial macrophages, neutrophils, cleaved caspase-3 and myofibroblasts

For neutrophils and macrophages, periodate lysine paraformaldehyde-fixed frozen tissue sections (6 μm) were stained with RB6-8C5 (anti-Gr-1) or F4/80 using a three-layer immunoperoxidase technique [20,24]. Neutrophil numbers were counted in ≥10 hpf per animal. As individual macrophages could not be reliably counted [20], ≥10 hpf were assessed per animal and cortical interstitial infiltrate scored as 0–3+ (0-equivalent to normal animals and the contralateral kidney of experimental animals, 1: 10–40% interstitium, 2: 40–70% interstitium, 3: >70% interstitium). For cleaved caspase-3, 4 μm paraffin-embedded sections were de-paraffinized (1 h, 60°C), followed by hydration and antigen retrieval. After blocking biotin and endogenous peroxidases, the sections were incubated with 10% swine serum (1 h, room temperature), then with a rabbit anti-human cleaved caspase-3 antibody (1:400, overnight, 4°C; Cell Signaling Technology, Danvers, MA, USA) that cross-reacts with mouse caspase-3 [25] and then with swine anti-rabbit biotin (1:100, 1 h, room temperature; Dako), followed by avidin/biotin (Dako) with 3,3′-diaminobenzidine. Ten consecutive hpf were assessed per animal, excluding glomeruli and large vessels, and results expressed as cells/hpf (c/hpf). Immunohistochemistry using Bouin's fixed tissue sections (4 μm) was used for α-SMA. The sections were stained with a peroxidase-conjugated mouse anti-human α-SMA antibody (1A4) using the Enhanced Polymer One-Step Staining reagent (Dako) [20] and then incubated overnight at 4°C; binding was detected using 3,3′-diaminobenzidine and the sections were counterstained with nuclear fast red (BDH Chemicals, Poole, UK). Dako negative control EPOS immunoglobulins-HRP were used as a negative control. Interstitial α-SMA accumulation was assessed by point counting.

Assessment of intrarenal chemokine, cytokine and collagen mRNA expression

The ribonuclease (RNAse) protection assay was performed as previously described [26]. Kidney RNA was extracted with a TRIzol reagent (Invitrogen, CA, USA) from randomly selected mice of a single experiment (n = 5–9 each group with UUO). Multiprobes incorporating [α-^{32}P]UTP were transcribed from two custom templates (RiboQuant System, Pharmingen), the first containing probes for ICAM-1 IL-1RI, E- selectin, TNF, VCAM-1, IL-1β, IL-1Ra, IL-18, F4/80, IFN-γ and macrophage migration inhibitory factor (MIF), the second containing probes for lymphotoxin-α, lymphotoxin-β, TNF, IL- 13, IFN-γ, type 1 procollagen α1 chain [α1(I) procollagen], TGF-β1, TGF-β2 and TGF-β3). Gene expression was normalized to the housekeeping gene L32.

For IL-1α mRNA, 1 μg RNA (n = 6–7 for each group with UUO) was treated with 1 unit of amplification grade DNase I (Invitrogen), then primed with 500 ng Oligo(dT)$_{12-18}$ (Roche, Mannheim, Germany) and reverse-transcribed (Super Script II, Invitrogen). For IL-1α (113 bp product) and β-actin (388 bp product) primers (Vector NTI software, Invitrogen), see the Supplementary data table. Real-time PCR was performed on a Rotor Gene RG-3000 (Corbett Research, NSW, Australia) using FastStart DNA Master, SYBR Green I (Roche). IL-1α and β-actin mRNA expression was quantified using serial dilutions of an exogenous standard, and IL-1α levels normalized to β-actin and expressed as arbitrary units. For connective tissue growth factor (CTGF) and α-SMA mRNA (n = 7–10 each group with UUO), TaqMan minor groove binder probes (Applied Biosystems 7500, Foster City, CA, USA) were linked to 6-carboxyfluorescein, and gene expression was analysed by real-time quantitative RT-PCR (TaqMan, Applied Biosystems) with 18S ribosomal RNA expression assessed (18S rRNA TaqMan Control Reagent kit) as a control. Results were expressed proportional to values obtained from WT mice obstructed kidneys.

Results

IL-1β and IL-1RI expression in obstructed kidneys of mice with UUO

IL-1 and IL-1R family gene expression was assessed in mice with obstructed kidneys 7 days after UUO. Both IL-1α and IL-1β mRNA were induced in kidneys of mice with disease (Table 1). In addition to induction of IL-1α and IL-1β expression, induction of the mRNA for IL-1RI and

Table 1. Expression of IL-1 and IL-1 receptor family mRNA in kidneys 1 week after unilateral ureteric ligation

	WT contralateral	WT UUO	Fold induction (× contralateral kidney)
IL-1α mRNA	0.13 ± 0.07	0.76 ± 0.55[a]	5.84
IL-1β mRNA	0.74 ± 0.08	2.79 ± 1.28[a]	3.77
IL-1RI mRNA	1.33 ± 0.21	3.76 ± 1.20[a]	2.82
IL-1Ra mRNA	0.54 ± 0.10	8.28 ± 1.54[a]	15.33

All values are expressed as mean ± SD, arbitrary units.
[a] $P < 0.05$.

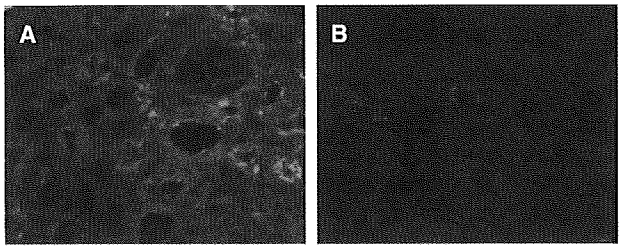

Fig. 1. Expression of IL-1RI in obstructed kidneys 7 days after undergoing unilateral ureteric ligation. In obstructed kidneys from C57BL/6 wild-type (WT) mice (**A**), IL-1RI expression was observed in the interstitium and at varying intensity within tubules. Signal was absent in obstructed kidneys from IL-1RI$^{-/-}$ mice (**B**). Original magnification ×200.

IL-1Ra was observed in obstructed kidneys. Immunofluorescent staining for IL-1RI revealed staining in areas of the interstitium and in tubules in obstructed kidneys from WT mice at Day 7 after UUO (Figure 1A), with minimal fluorescence in obstructed kidneys from IL-1RI$^{-/-}$ mice (Figure 1B) as a negative control.

Renal interstitial fibrosis is reduced in the absence of the IL-1RI

Compared with the unobstructed contralateral kidney (Figure 2A and B), obstructed kidneys from 7-day UUO mice demonstrated increased picrosirius red staining and increased matrix production (Figure 2C and D). Histologically, mice deficient in either IL-1β or IL-1RI exhibited reduced injury with reduced picrosirius red staining (Figures 2E–H and 3A). Analyses of the biochemical accumulation of collagen (Figure 3B) and α1(I) procollagen mRNA expression (Figure 3C) confirmed that IL-1RI$^{-/-}$ mice were relatively protected from collagen accumulation in interstitial fibrosis, although values for IL-1β$^{-/-}$ mice were not different from those for WT mice.

Endogenous IL-1/IL-1RI interactions enhance TGF-β and CTGF mRNA expression

To understand why IL-1/IL-1RI interactions play a profibrotic role *in vivo* in UUO, the expression of the three isoforms of TGF-β and of CTGF, a downstream effector of TGF-β, was measured. Compared with WT, IL-1RI$^{-/-}$-obstructed kidneys expressed less TGF-β1 mRNA and less CTGF mRNA (Figure 4). Apparent reductions in TGF-β2 and TGF-β3 did not reach statistical significance. In IL-1β$^{-/-}$ mice, TGF-β1 mRNA and CTGF mRNA were similar to WT values.

Renal tubulointerstitial apoptosis and myofibroblast accumulation

Apoptosis is important in the development of renal fibrosis due to obstruction. Immunohistochemistry revealed significant apoptosis, determined by cleaved caspase-3 positive tubular and interstitial cells, in obstructed kidneys from WT mice (Figure 5A and G). IL-1RI$^{-/-}$ mice were protected from apoptosis, with fewer cleaved caspase-3-positive cells

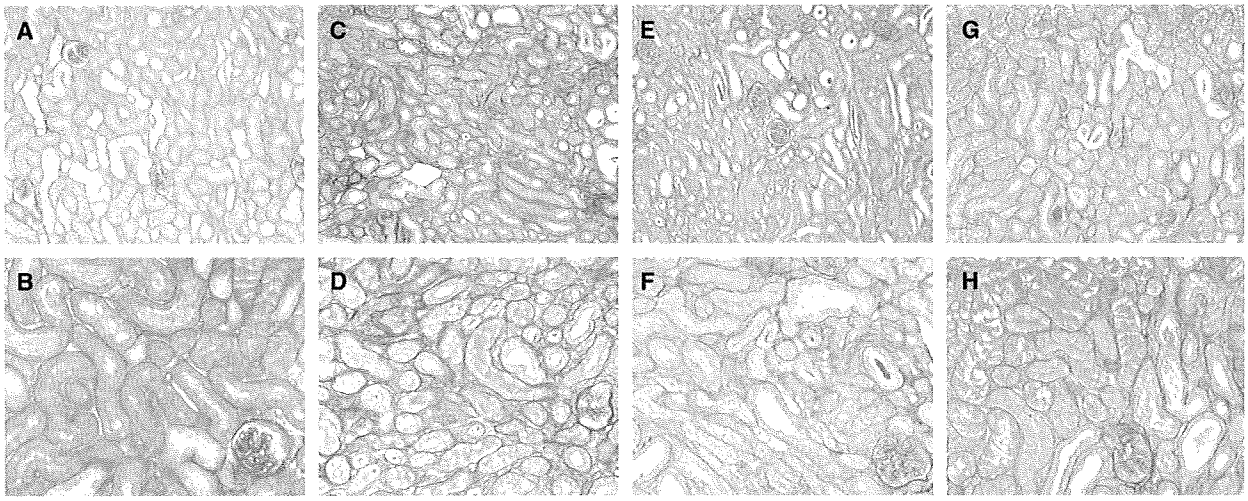

Fig. 2. Renal histopathology of C57BL/6 wild-type (WT) mice, IL-1β$^{-/-}$ mice and IL-1RI$^{-/-}$ mice 7 days after undergoing unilateral ureteric obstruction. Contralateral kidneys from WT mice demonstrated no abnormalities (**A** and **B**). Seven days after ureteric ligation, WT mice demonstrated tubular dilatation, interstitial expansion and increased matrix expression (red, **C** and **D**). In IL-1β$^{-/-}$ mice, these changes were relatively less severe (**E** and **F**). Mice deficient in the IL-1RI demonstrated substantial projection from injury (**G** and **H**). Picrosirius red staining of paraffin-fixed sections. All photomicrographs are taken of the outer cortex. Original magnifications ×100 (**A**, **C**, **E** and **G**) and ×200 (**B**, **D**, **F** and **H**).

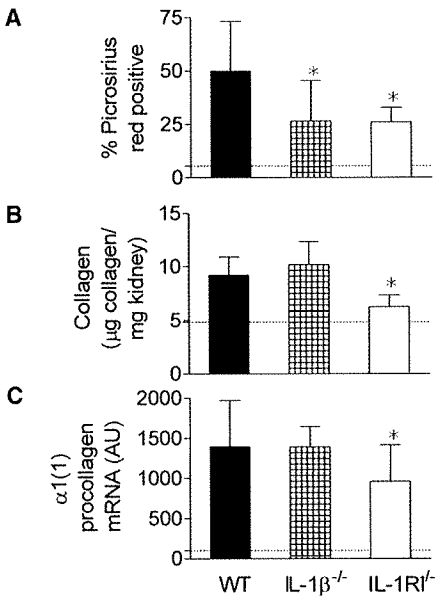

Fig. 3. Collagen accumulation in obstructed kidneys 7 days after undergoing unilateral ureteric ligation. Seven days after unilateral ureteric ligation, C57BL/6 wild-type (WT) mice exhibited increased picrosirius red staining (**A**), increased collagen accumulation measured biochemically by hydroxyproline assay (**B**) and increased expression of mRNA for the α1 chain of type I procollagen (**C**). Dotted lines represent values from the contralateral kidneys. IL-1RI$^{-/-}$ mice were relatively protected from fibrosis in all three indices, while IL-1β$^{-/-}$ mice had less cortical interstitial expansion, but no change in biochemically assessed collagen accumulation or α1(I) procollagen mRNA expression. *$P < 0.05$ versus WT obstructed kidneys.

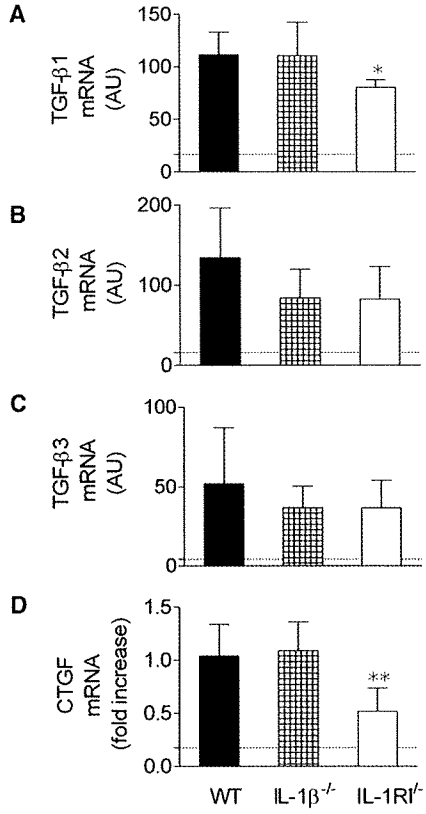

Fig. 4. Pro-fibrotic growth factor mRNA expression in obstructed kidneys 7 days after undergoing unilateral ureteric ligation. Compared with obstructed kidneys from C57BL/6 wild-type (WT) mice, TGF-β1 mRNA expression was significantly reduced in IL-1RI$^{-/-}$ mice (**A**). There was a trend to reduced TGF-β2 mRNA in both IL-1β$^{-/-}$ mice and IL-1RI$^{-/-}$ mice that was not significant (**B**). There was no change in TGF-β3 mRNA expression (**C**). CTGF mRNA expression was reduced compared with WT or IL-1β$^{-/-}$ mice in the absence of the IL-1RI (**D**). Dotted lines represent values for contralateral kidneys of C57BL/6 WT mice. *$P < 0.05$ versus WT obstructed kidneys, **$P < 0.01$ versus WT or IL-1β$^{-/-}$ obstructed kidneys.

present in the tubulointerstitium of obstructed kidneys (Figure 5C), but IL-1β deficiency did not result in reduced apoptosis (Figure 5B). As a marker for epithelial myofibroblast transformation, α-SMA was assessed (Figure 5D–F, H and I). Compared with WT mice (Figure 5D), IL-1β$^{-/-}$ mice had similar α-SMA mRNA expression and a similar proportion of the interstitium covered by α-SMA-expressing cells (Figure 5E). In IL-1RI$^{-/-}$ mice, the reduction in α-SMA mRNA expression fell just short of statistical significance (ANOVA, $P = 0.054$).

Macrophage and neutrophil infiltration is unaffected in the absence of either IL-1β or IL-1RI

Seven days after the induction of UUO, WT mice exhibited a significant infiltrate of F4/80+ macrophages in the tubulointerstitium (Figure 6A and D). The extent of this macrophage infiltrate was unaltered in the absence of either IL-1β or IL-1RI (Figure 6 B–D). To confirm this negative finding, intrarenal expression of F4/80 mRNA was similar in all three groups of mice at 7 days (Figure 6E). Neutrophil accumulation was also unaffected by IL-1β or IL-1RI deficiency (WT 2.9 ± 1.0, IL-1β$^{-/-}$ 2.4 ± 1.2, IL-1RI$^{-/-}$ 3.5 ± 0.71 cells/hpf).

Expression of pro-inflammatory cytokines and adhesion molecules in IL-1β$^{-/-}$ and IL-1RI$^{-/-}$ mice

As IL-1 can induce other proinflammatory mediators, proinflammatory cytokines and adhesion molecules were studied in obstructed kidneys from WT, IL-1β$^{-/-}$ and IL-1RI$^{-/-}$ mice (Table 2). Induction of these mRNA species was observed in the obstructed kidney (compared with the contralateral kidney, except for MIF mRNA, paradoxically decreased). IL-1β or IL-1RI deficiency did not affect expression of TNF, MIF or IL-18 mRNA. Compared with obstructed kidneys from WT mice, IFN-γ mRNA expression was decreased in obstructed kidneys from both IL-1β$^{-/-}$ and IL-1RI$^{-/-}$ mice. Consistent with the lack of the effect of endogenous IL-1 on macrophage accumulation, in obstructed kidneys, mRNA for E-selectin, ICAM-1 and VCAM-1 was unaffected by the absence of either IL-1β or IL-1RI.

Changes in IL-1/IL-1R family gene expression in IL-1β$^{-/-}$ and IL-1RI$^{-/-}$ mice

To assess whether up- or downregulation of IL-1α, IL-1RI or IL-1Ra in IL-1β$^{-/-}$ mice explains the more significant protection in IL-1RI$^{-/-}$ mice, expression of IL-1α, IL-1β, IL-1RI and IL-1Ra was assessed in IL-1β$^{-/-}$ and IL-1RI$^{-/-}$ mice (Table 3). No compensatory changes that would account for this difference were observed.

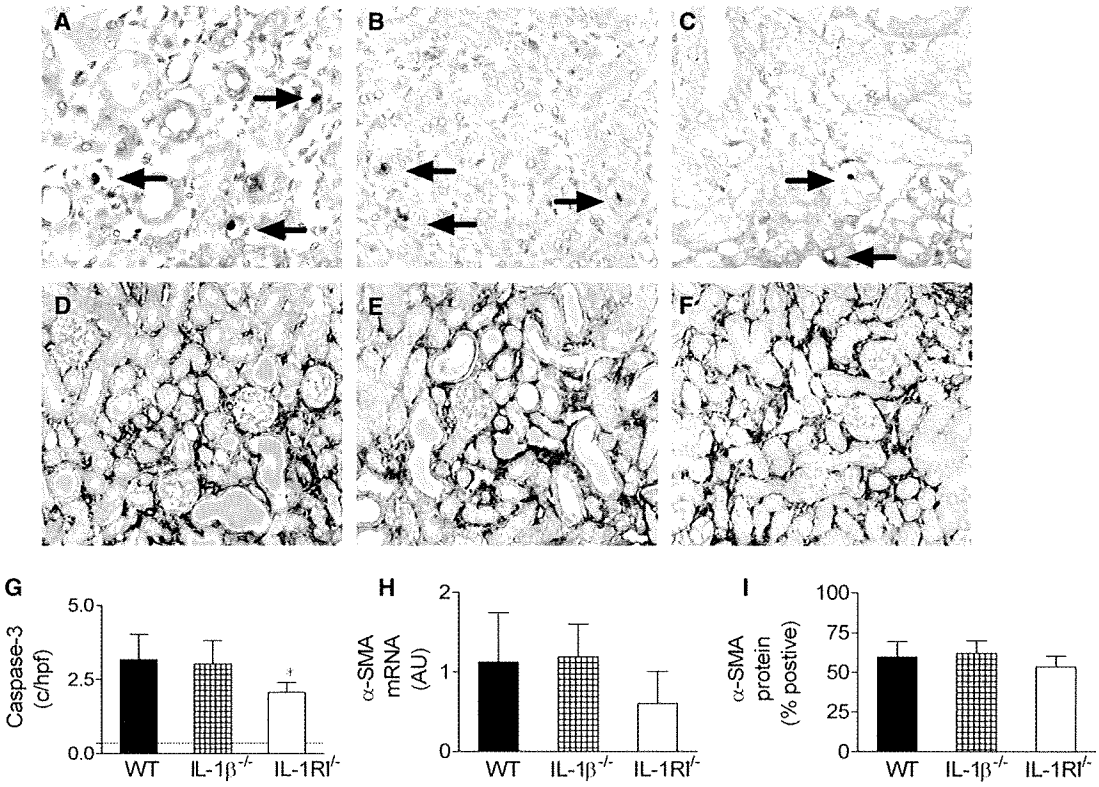

Fig. 5. Apoptosis and expression of α-SMA in obstructed kidneys 7 days after unilateral ureteric ligation. Photomicrographs of apoptotic cells, assessed by immunostaining of cleaved caspase-3 positive cells (arrowed) in WT mice (**A**), with similar numbers in IL-1β$^{-/-}$ mice (**B**) and reduced numbers of IL-1RI$^{-/-}$ mice (**C**). Similar proportions of tissues positive for α-SMA were present in all three groups of mice (WT, D; IL-1β$^{-/-}$ E and IL-1RI F). Quantitation of these changes shows a reduced number of apoptotic cells in IL-1RI$^{-/-}$ mice (**G**). The dotted line represents the number of cleaved caspase-3-positive c/hpf in contralateral kidneys of wild-type (WT) mice. Compared with obstructed kidneys of C57BL/6 WT mice, there was a trend to reduced α-SMA mRNA expression (**H**) ($P = 0.054$, ANOVA) in obstructed kidneys of IL-1RI$^{-/-}$ mice. The proportion of the tubulointerstitium covered with α-SMA-positive cells (point counting) was similar in all three groups (I). *$P < 0.05$ versus WT obstructed kidneys. Original magnifications × 400 (**A**– **C**) and ×200 (**D**– **F**).

In obstructed kidneys of IL-1β$^{-/-}$ mice, neither IL-1α nor IL-1RI was further up-regulated. IL-1Ra, potentially protective in UUO, was not downregulated in IL-1β$^{-/-}$ mice. In obstructed kidneys of IL-1RI$^{-/-}$ mice, IL-1β was not upregulated compared with WT. IL-1α mRNA was not significantly increased in IL-1RI$^{-/-}$ mice over WT, but in IL-1RI$^{-/-}$ mice, mRNA for IL-1Ra was increased over WT values.

Catch-up in interstitial fibrosis at 2 weeks in IL-1RI$^{-/-}$ mice

To determine whether IL-1RI deficiency results in lasting protection from interstitial fibrosis, IL-1RI$^{-/-}$ mice were studied 2 weeks after UUO. Histologically, fibrosis had progressed in WT mice and appearances in IL-1RI$^{-/-}$ mice were similar to WT (Figure 7A–D). This catch-up in disease was confirmed by measurement of indices of renal fibrosis. With the exception of a trend to reduced α1(I) procollagen mRNA expression ($P = 0.16$), values were similar in 2-week obstructed kidneys in WT and IL-1RI$^{-/-}$ mice (Figure 8). Analysis of other mediators of fibrosis and inflammation (Table 4) showed no difference in TGF-β mRNA, α-SMA accumulation or adhesion molecule expression. Scoring of infiltrating F4/80+ macrophages was identical, but compared with obstructed WT kidneys at 2 weeks, F4/80 mRNA was reduced in IL-1RI$^{-/-}$ mice. The reduced IFN-γ mRNA observed at 1 week was no longer apparent and both MIF and IL-18 mRNA were increased in IL-1RI$^{-/-}$ mice.

Discussion

Interactions between IL-1 and the IL-1RI are important in inflammatory renal disease. Human data suggest that polymorphisms in the IL-1 gene cluster, specifically, the variable-number-of-tandem-repeats polymorphism in the gene encoding IL-1Ra and a single-nucleotide polymorphism in the IL-1α promoter, were associated with an increased risk of end-stage renal failure [27]. We hypothesized that IL-1 and the type I IL-1 receptor contribute to experimental progressive renal disease. As we expected, mRNA for the IL-1 family, both proinflammatory (IL-1α, IL-1β and IL-1RI) and anti-inflammatory (IL-1Ra), were upregulated by 7 days after UUO. Previous studies have demonstrated upregulation of IL-1β and IL-1RI at an mRNA and/or protein level [17], and *in vitro* studies have demonstrated that renal fibroblasts produce both IL-1α and IL-1β [12]. The current studies tested the hypotheses that these interactions are important in obstructive uropathy-induced renal fibrosis. They demonstrate that IL-1RI plays

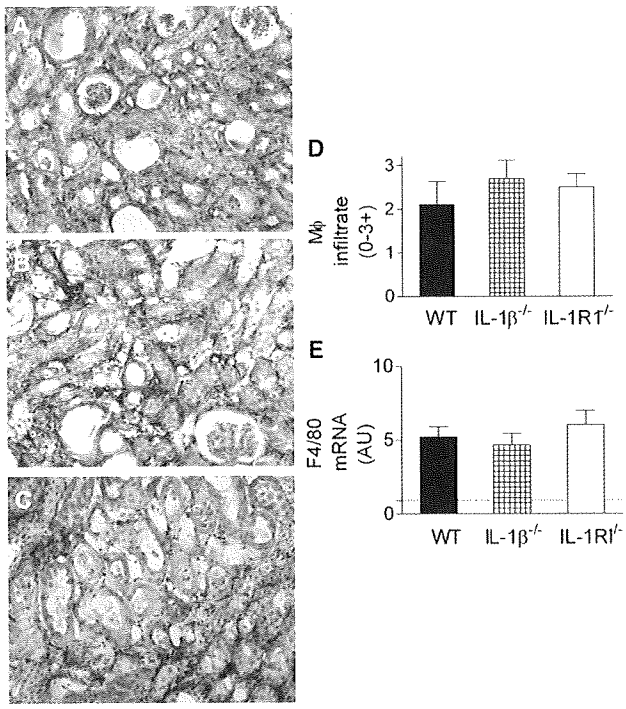

Fig. 6. Macrophage infiltration and F4/80 gene expression in obstructed kidneys 7 days after undergoing unilateral ureteric ligation There was a significant F4/80+ macrophage infiltrate (periodate lysine paraformaldehyde fixed, frozen tissue section, black reaction product) in C57BL/6 wild-type (WT) mice (**A**), IL-1β$^{-/-}$ mice (**B**) and IL-1RI$^{-/-}$ mice (**C**). There was no difference in the extent of the infiltrate when assessed semiquantitatively (**D**), and the expression of F4/80 mRNA in obstructed kidneys was similar in all groups (**E**). Original magnification for panels (**A**–**C**) ×200.

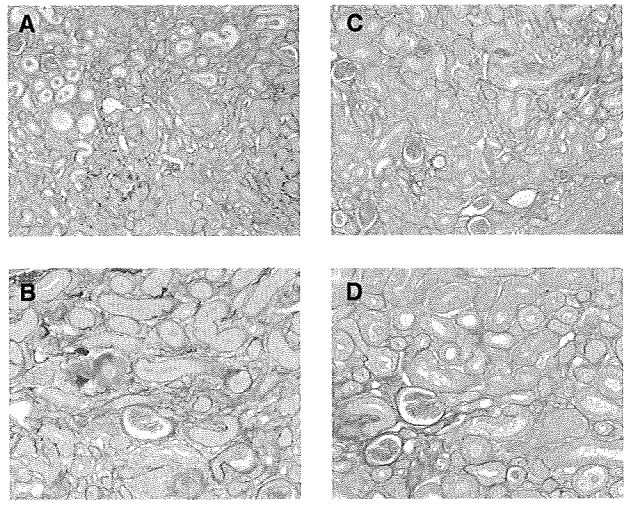

Fig. 7. Renal histopathology of C57BL/6 wild-type (WT) mice and IL-1RI$^{-/-}$ mice 2 weeks after undergoing unilateral ureteric obstruction. Two weeks after ureteric ligation, WT mice (**A** and **B**) demonstrated increased interstitial fibrosis compared with 1-week samples (red, **C** and **D**). Mice deficient in the IL-1RI demonstrated similar severity of disease (**C** and **D**). All photomicrographs are taken of the outer cortex. Picrosirius red staining of paraffin fixed sections. Original magnifications ×100 (**A** and **C**) and ×200 (**B** and **D**).

Table 2. Expression of proinflammatory cytokine and adhesion molecule genes at 1 week in kidneys of wild-type (WT), IL-1β$^{-/-}$ and IL-R1$^{-/-}$ mice with unilateral ureteric obstruction

	WT contralateral	WT UUO	IL-1β$^{-/-}$ UUO	IL-1R1$^{-/-}$ UUO
TNF	3.2 ± 0.2	10.4 ± 3.8	14.0 ± 4.0	13.3 ± 3.8
IL-18	0.60 ± 0.13	1.76± 0.77	2.82± 0.83	2.97± 1.42
MIF	749 ± 48	369 ± 69	335 ± 57	396 ± 35
IFN-γ	2.0 ± 1.0	12.1 ± 1.5	6.2 ± 1.2[a]	5.0 ± 1.9[a]
E-selectin	0.68 ± 0.05	2.34 ± 0.49	2.40 ± 0.40	2.17 ± 0.74
ICAM-1	3.57 ± 0.31	12.3 ± 5.2	13.3 ± 3.6	11.6 ± 7.4
VCAM-1	4.5 ± 0.5	80.4± 13.4	87.6 ± 13.9	99.0 ± 26.7

All values are expressed as mean ± SD.
[a]$P < 0.001$ versus WT UUO.

Table 3. Comparison of the expression of mRNA for IL-1 family members in obstructed kidneys from wild-type (WT), IL-1β$^{-/-}$ and IL-1RI$^{-/-}$ mice

	WT UUO	IL-1β$^{-/-}$ UUO	IL-1RI$^{-/-}$ UUO
IL-1α mRNA	0.77 ± 0.56	0.79 ± 0.64	1.08 ± 0.35
IL-1β mRNA	2.79 ± 1.28	–	2.49 ± 1.05
IL-1RI mRNA	3.75 ± 1.20	4.02 ± 1.06	–
IL-1Ra mRNA	8.28 ± 1.54	8.66 ± 1.59	14.36 ± 2.48[a]

All values are expressed as mean ± SD, arbitrary units. Data for WT mice were also presented in Table 1.
[a]$P < 0.001$ versus WT UUO.

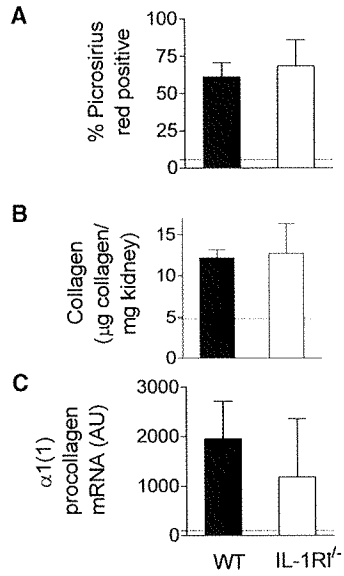

Fig. 8. Collagen accumulation in obstructed kidneys 2 weeks after undergoing unilateral ureteric ligation. Two weeks after unilateral ureteric ligation, collagen accumulation in IL-1RI$^{-/-}$ mice was similar to that in C57BL/6 wild-type (WT) mice assessed by picrosirius red staining (**A**), biochemical assessment of collagen accumulation (**B**) and expression of mRNA for the α1 chain of type I procollagen (**C**, $P = 0.16$). Dotted lines represent values from contralateral kidneys.

a profibrotic role in obstructive uropathy by promoting TGF-β1 mRNA expression and its downstream effects, including the induction of CTGF and expression of type I collagen mRNA and protein, findings supported by reduced apoptosis in IL-1RI$^{-/-}$ mice. IL-1 can affect macrophages, particularly by enhancing their recruitment into the kidney, and in overtly immune-mediated experimental renal injury,

Table 4. Fibrotic and inflammatory parameters after 2 weeks in kidneys subjected to unilateral ureteric obstruction in genetically normal wild-type (WT) mice and IL-1RI$^{-/-}$ mice

	WT	IL-1RI$^{-/-}$
TGF-β1 mRNA	57.1 ± 28.0	54.9 ± 30.0
TGF-β2 mRNA	59.8 ± 30.6	46.8 ± 30.1
TGF-β3 mRNA	47.3 ± 22.9	31.3 ± 22.0
α-SMA (%)	52.8 ± 20.0	35.9 ± 18.5
Macrophages (0–3+)	2.7 ± 0.2	2.7 ± 0.7
F4/80 mRNA	7.0 ± 0.8	4.4 ± 0.7[b]
TNF mRNA	10.9 ± 1.6	12.4 ± 2.0
Neutrophils (c/hpf)	1.6 ± 1.2	2.6 ± 1.2
IL-18 mRNA	1.49 ± 0.23	2.18 ± 0.33[b]
MIF mRNA	142 ± 35	221 ± 47[a]
IFN-γ mRNA	5.34 ± 2.44	4.63 ± 4.22
E-selectin mRNA	3.51 ± 0.28	3.20 ± 0.67
ICAM-1 mRNA	27.3 ± 6.3	24.2 ± 6.9
VCAM-1 mRNA	99.3 ± 14.5	119 ± 30.6

Except as indicated, all values are expressed as mean ± SD, arbitrary units. [a]$P < 0.01$, [b]$P < 0.001$.

IL-1 does affect macrophages. However, our studies found no effects on macrophage or neutrophil infiltration or expression of adhesion molecules, confirming that IL-1 acts on TGF-β, independent of effects on immune cells.

The current studies, supporting a profibrotic role for the IL-1RI in renal fibrosis, are concordant with *in vitro* studies [10–13] and *in vivo* studies using IL-1Ra [17]. There are several mechanisms by which this can occur, including adhesion molecule induction, enhancement of inflammatory macrophage recruitment, macrophage activation or induction of TGF-β, well recognized as an important profibrotic growth factor [28]. Some studies in experimental renal disease have suggested that IL-1/IL-1RI interactions are pathogenetic due to their effects on leukocyte recruitment and accumulation [17,29–31]. In our studies, no change in macrophage infiltration was observed. At least one other study has inhibited IL-1 and found no alterations in the recruitment of macrophages, unless other cytokines were concurrently neutralized [32]. It is likely that the nature and intensity of the disease (in the current studies, complete ureteric obstruction) can engage other mediators of leukocyte recruitment in an IL-1RI-independent manner. IL-1 does have the capacity to promote macrophage accumulation and increase the expression of adhesion molecules, and deficiency of leukocyte adhesion molecules limits fibrosis in newborn mice [33]. However, E-selectin, ICAM-1 or VCAM-1 mRNA expression was unchanged in the absence of IL-1β or IL-1RI. Not all studies have reported that endogenous IL-1 affects adhesion molecules, suggesting that the affects of IL-1 on adhesion molecules may be stimulus specific. For example, in MRL/*lpr* mice, IL-1 neutralization did not alter ICAM-1 expression [34]. The effects of IL-1/IL-1RI on the production of other proinflammatory molecules revealed that the expression of TNF, MIF and IL-18 mRNA was unaffected, but IFN-γ mRNA expression was decreased. While IFN-γ activates macrophages to enhance inflammation, potentially increasing injury and downstream fibrosis, it can also antagonize TGF-β-induced collagen gene expression [35]. The net effect of changes in IFN-γ expression, particularly in renal diseases independent of adaptive immune responses, is uncertain [36–38].

In vitro studies using primary cultures of human proximal tubular cells or cortical fibroblasts suggest that IL-1β's profibrotic effects are TGF-β mediated [10,13]. IL-1α could promote fibrosis by enhancing epithelial myofibroblast transformation in a TGF-β-dependent manner [8]. The current studies demonstrate that *in vivo*, IL-1/IL-1RI interactions promote TGF-β, CTGF and α-SMA gene expression consistent with these and other *in vitro* studies [8–10,13]. In addition, reduced apoptosis in IL-1RI$^{-/-}$ mice is likely to have been due to reduced TGF-β [39]. IL-1β has been previously demonstrated in infiltrating cells and in tubular cells in both experimental and human renal disease [40–42]. A number of cell types, both immune cells and resident tissue cells, have the capacity to express IL-1α, IL-1β and the IL-1R. Functional studies using chimeric mice in experimental glomerulonephritis demonstrated that interactions between leukocyte-derived IL-1β and renal tissue cell-expressed IL-1RI are important in renal injury [43,44]. From our studies it is not possible to ascertain the dominant cellular source of IL-1 in UUO, but IL-1's effects are likely to be through IL-1RI on both tubular cells and fibroblasts.

IL-1RI-deficient mice were more protected than IL-1β$^{-/-}$ mice. There were no changes in IL-1α, IL-1RI or IL-1Ra mRNA in IL-1β$^{-/-}$ mice, suggesting that IL-1β$^{-/-}$ mice did not develop compensatory changes in the developmental absence of IL-1β. Incidentally, IL-1RI$^{-/-}$ mice did show IL-Ra increased expression, but as the IL-1RI is the only signalling receptor for IL-1α and IL-1β, this change is unlikely to be biologically significant. IL-1α is expressed in diseased human kidneys [42], has pro-inflammatory effects on renal tubular cells [45] and may induce epithelial myofibroblast transformation [8]. Taking these data into account, the probable explanation for the greater protection in mice deficient in IL-1RI is that IL-1α plays a pathogenetic role in disease.

To determine the absolute requirement for IL-1RI, the effects of IL-1RI deficiency were assessed 2 weeks after UUO. By this time, IL-1RI$^{-/-}$ mice had developed similar disease to that of WT mice, suggesting significant catch-up in injury. Although there was a trend towards reduced α1(I) procollagen mRNA, collagen accumulation and histological injury were similar, as was the expression of TGF-β isoforms. These findings demonstrate that, at least in this model of fibrosis involving an ongoing and pervasive fibrotic stimulus (i.e. ureteric obstruction with ongoing mechanical stress and inflammation), other pathways that lead to TGF-β production and fibrosis are able to, with time, compensate for the absence of IL-1/IL-1R interactions.

IL-1 has the capacity to influence adaptive immune responses, which can themselves cause fibrosis. Although reducing inflammation by modulating adaptive immune responses reduces collagen accumulation [26], renal fibrosis induced by UUO is T cell (and adaptive immunity) independent [46]. The potential for deletion/inhibition of IL-1 or IL-1RI to modulate the direction of the adaptive immune response, while important in some renal diseases [29,43,47], is not relevant to these studies. The current studies examine UUO-induced renal fibrosis and cannot necessarily be generalized to all forms of progressive renal disease.

However, there is functional evidence in other *in vivo* models of progressive renal disease and other organ systems that IL-1 is important in fibrosis. This evidence includes IL-1Ra offering protection from progressive renal disease in pathological adaptive immune responses affecting the kidney [30], improvement in experimental pulmonary fibrosis after IL-1Ra [48] and radiation-induced dermal fibrosis [49]. In summary, in renal fibrosis induced by UUO, interactions between endogenous IL-1 (IL-1α and IL-1β) and the IL-1RI are profibrotic. Their effects are mediated through the production and effects of TGF-β and not by enhancing macrophage recruitment, but at least in UUO, the protective effects of IL-1RI deficiency do not persist when fibrosis progresses.

Supplementary data

Supplementary data are available online at http://ndt.oxfordjournals.org.

Acknowledgements. The assistance of Ms Alice Wright is acknowledged. These studies were supported by a Programme Grant from the NHMRC of Australia (334067).

Conflicts of interest statement. None declared.

References

1. Eddy AA. Progression in chronic kidney disease. *Adv Chronic Kidney Dis* 2005; 12: 353–365
2. Harris RC, Neilson EG. Toward a unified theory of renal progression. *Annu Rev Med* 2006; 57: 365–380
3. Liu Y. Renal fibrosis: new insights into the pathogenesis and therapeutics. *Kidney Int* 2006; 69: 213–217
4. Dinarello CA. Biologic basis for interleukin-1 in disease. *Blood* 1996; 87: 2095–2147
5. Arend WP. The balance between IL-1 and IL-1Ra in disease. *Cytokine Growth Factor Rev* 2002; 13: 323–340
6. Arend WP, Malyak M, Guthridge CJ *et al.* Interleukin-1 receptor antagonist: role in biology. *Annu Rev Immunol* 1998; 16: 27–55
7. Colotta F, Dower SK, Sims JE *et al.* The type II 'decoy' receptor: a novel regulatory pathway for interleukin 1. *Immunol Today* 1994; 15: 562–566
8. Fan JM, Huang XR, Ng YY *et al.* Interleukin-1 induces tubular epithelial-myofibroblast transdifferentiation through a transforming growth factor-beta1-dependent mechanism *in vitro*. *Am J Kidney Dis* 2001; 37: 820–831
9. Phillips AO, Topley N, Steadman R *et al.* Induction of TGF-beta 1 synthesis in D-glucose primed human proximal tubular cells by IL-1 beta and TNF alpha. *Kidney Int* 1996; 50: 1546–1554
10. Vesey DA, Cheung CW, Cuttle L *et al.* Interleukin-1beta induces human proximal tubule cell injury, alpha-smooth muscle actin expression and fibronectin production. *Kidney Int* 2002; 62: 31–40
11. Lonnemann G, Shapiro L, Engler-Blum G *et al.* Cytokines in human renal interstitial fibrosis: I. Interleukin-1 is a paracrine growth factor for cultured fibrosis-derived kidney fibroblasts. *Kidney Int* 1995; 47: 837–844
12. Lonnemann G, Engler-Blum G, Muller GA *et al.* Cytokines in human renal interstitial fibrosis: II. Intrinsic interleukin (IL)-1 synthesis and IL-1-dependent production of IL-6 and IL-8 by cultured kidney fibroblasts. *Kidney Int* 1995; 47: 845–854
13. Vesey DA, Cheung C, Cuttle L *et al.* Interleukin-1beta stimulates human renal fibroblast proliferation and matrix protein production by means of a transforming growth factor-beta-dependent mechanism. *J Lab Clin Med* 2002; 140: 342–350
14. Chevalier RL. Obstructive nephropathy: towards biomarker discovery and gene therapy. *Nat Clin Pract Nephrol* 2006; 2: 157–168
15. Bascands JL, Schanstra JP. Obstructive nephropathy: insights from genetically engineered animals. *Kidney Int* 2005; 68: 925–937
16. Docherty NG, O'Sullivan OE, Healy DA *et al.* Evidence that inhibition of tubular cell apoptosis protects against renal damage and development of fibrosis following ureteric obstruction. *Am J Physiol Renal Physiol* 2006; 290: F4–F13
17. Yamagishi H, Yokoo T, Imasawa T *et al.* Genetically modified bone marrow-derived vehicle cells site specifically deliver an anti-inflammatory cytokine to inflamed interstitium of obstructive nephropathy. *J Immunol* 2001; 166: 609–616
18. Horai R, Asano M, Sudo K *et al.* Production of mice deficient in genes for interleukin (IL)-1alpha, IL-1beta, IL-1alpha/beta, and IL-1 receptor antagonist shows that IL-1beta is crucial in turpentine-induced fever development and glucocorticoid secretion. *J Exp Med* 1998; 187: 1463–1475
19. Labow M, Shuster D, Zetterstrom M *et al.* Absence of IL-1 signaling and reduced inflammatory response in IL-1 type I receptor-deficient mice. *J Immunol* 1997; 159: 2452–2461
20. Edgtton KL, Gow RM, Kelly DJ *et al.* Plasmin is not protective in experimental renal interstitial fibrosis. *Kidney Int* 2004; 66: 68–76
21. Yu HC, Burrell LM, Black MJ *et al.* Salt induces myocardial and renal fibrosis in normotensive and hypertensive rats. *Circulation* 1998; 98: 2621–2628
22. Ma J, Nishimura H, Fogo A *et al.* Accelerated fibrosis and collagen deposition develop in the renal interstitium of angiotensin type 2 receptor null mutant mice during ureteral obstruction. *Kidney Int* 1998; 53: 937–944
23. Bergman I, Loxley R. Two improved and simplified methods for the spectrophotometric determination of hyroxproline. *Anal Chem* 1963; 35: 1961–1965
24. Kitching AR, Turner AL, Semple T *et al.* Experimental autoimmune anti-glomerular basement membrane glomerulonephritis: a protective role for IFN-gamma. *J Am Soc Nephrol* 2004; 15: 1764–1774
25. Ma FY, Flanc RS, Tesch GH *et al.* A pathogenic role for c-Jun amino-terminal kinase signaling in renal fibrosis and tubular cell apoptosis. *J Am Soc Nephrol* 2007; 18: 472–484
26. Kitching AR, Turner AL, Wilson GR *et al.* IL-12p40 and IL-18 in crescentic glomerulonephritis: IL-12p40 is the key Th1-defining cytokine chain, whereas IL-18 promotes local inflammation and leukocyte recruitment. *J Am Soc Nephrol* 2005; 16: 2023–2033
27. Wetmore JB, Hung AM, Lovett DH *et al.* Interleukin-1 gene cluster polymorphisms predict risk of ESRD. *Kidney Int* 2005; 68: 278–284
28. Border WA, Noble NA. Transforming growth factor beta in tissue fibrosis. *N Engl J Med* 1994; 331: 1286–1292
29. Lan HY, Nikolic-Paterson DJ, Zarama M *et al.* Suppression of experimental crescentic glomerulonephritis by the interleukin-1 receptor antagonist. *Kidney Int* 1993; 43: 479–485
30. Lan HY, Nikolic-Paterson DJ, Mu W *et al.* Interleukin-1 receptor antagonist halts the progression of established crescentic glomerulonephritis in the rat. *Kidney Int* 1995; 47: 1303–1309
31. Haq M, Norman J, Saba SR *et al.* Role of IL-1 in renal ischemic reperfusion injury. *J Am Soc Nephrol* 1998; 9: 614–619
32. Zwerina J, Hayer S, Tohidast-Akrad M *et al.* Single and combined inhibition of tumor necrosis factor, interleukin-1, and RANKL pathways in tumor necrosis factor-induced arthritis: effects on synovial inflammation, bone erosion, and cartilage destruction. *Arthritis Rheum* 2004; 50: 277–290
33. Lange-Sperandio B, Cachat F, Thornhill BA *et al.* Selectins mediate macrophage infiltration in obstructive nephropathy in newborn mice. *Kidney Int* 2002; 61: 516–524
34. McHale JF, Harari OA, Marshall D *et al.* TNF-alpha and IL-1 sequentially induce endothelial ICAM-1 and VCAM-1 expression in MRL/lpr lupus-prone mice. *J Immunol* 1999; 163: 3993–4000
35. Varga J, Olsen A, Herhal J *et al.* Interferon-gamma reverses the stimulation of collagen but not fibronectin gene expression by

transforming growth factor-beta in normal human fibroblasts. *Eur J Clin Invest* 1990; 20: 487–493
36. Montinaro V, Hevey K, Aventaggiato L *et al.* Extrarenal cytokines modulate the glomerular response to IgA immune complexes. *Kidney Int* 1992; 42: 341–353
37. Johnson RJ, Lombardi D, Eng E *et al.* Modulation of experimental mesangial proliferative nephritis by interferon-gamma. *Kidney Int* 1995; 47: 62–69
38. Oldroyd SD, Thomas GL, Gabbiani G *et al.* Interferon-gamma inhibits experimental renal fibrosis. *Kidney Int* 1999; 56: 2116–2127
39. Miyajima A, Chen J, Lawrence C *et al.* Antibody to transforming growth factor-beta ameliorates tubular apoptosis in unilateral ureteral obstruction. *Kidney Int* 2000; 58: 2301–2313
40. Tipping PG, Lowe MG, Holdsworth SR. Glomerular interleukin 1 production is dependent on macrophage infiltration in anti-GBM glomerulonephritis. *Kidney Int* 1991; 39: 103–110
41. Tesch GH, Yang N, Yu H *et al.* Intrinsic renal cells are the major source of interleukin-1 beta synthesis in normal and diseased rat kidney. *Nephrol Dial Transplant* 1997; 12: 1109–1115
42. Waldherr R, Noronha IL, Niemir Z *et al.* Expression of cytokines and growth factors in human glomerulonephritides. *Pediatr Nephrol* 1993; 7: 471–478
43. Timoshanko JR, Kitching AR, Iwakura Y *et al.* Contributions of IL-1beta and IL-1alpha to crescentic glomerulonephritis in mice. *J Am Soc Nephrol* 2004; 15: 910–918
44. Timoshanko JR, Kitching AR, Iwakura Y *et al.* Leukocyte-derived interleukin-1beta interacts with renal interleukin-1 receptor I to promote renal tumor necrosis factor and glomerular injury in murine crescentic glomerulonephritis. *Am J Pathol* 2004; 164: 1967–1977
45. Boswell RN, Yard BA, Schrama E *et al.* Interleukin 6 production by human proximal tubular epithelial cells *in vitro*: analysis of the effects of interleukin-1 alpha (IL-1 alpha) and other cytokines. *Nephrol Dial Transplant* 1994; 9: 599–606
46. Shappell SB, Gurpinar T, Lechago J *et al.* Chronic obstructive uropathy in severe combined immunodeficient (SCID) mice: lymphocyte infiltration is not required for progressive tubulointerstitial injury. *J Am Soc Nephrol* 1998; 9: 1008–1017
47. Holdsworth SR, Kitching AR, Tipping PG. Th1 and Th2 T helper cell subsets affect patterns of injury and outcomes in glomerulonephritis. *Kidney Int* 1999; 55: 1198–1216
48. Piguet PF, Vesin C, Grau GE *et al.* Interleukin 1 receptor antagonist (IL-1ra) prevents or cures pulmonary fibrosis elicited in mice by bleomycin or silica. *Cytokine* 1993; 5: 57–61
49. Liu W, Ding I, Chen K *et al.* Interleukin 1beta (IL1B) signaling is a critical component of radiation-induced skin fibrosis. *Radiat Res* 2006; 165: 181–191

Received for publication: 7.1.09; Accepted in revised form: 20.4.09

Nephrol Dial Transplant (2009) 24: 1162–1169
doi: 10.1093/ndt/gfn630
Advance Access publication 17 November 2008

Involvement of asymmetric dimethylarginine (ADMA) in tubulointerstitial ischaemia in the early phase of diabetic nephropathy

Ryo Shibata[1], Seiji Ueda[1], Sho-ichi Yamagishi[2], Yusuke Kaida[1], Yuriko Matsumoto[1], Kei Fukami[1], Ayako Hayashida[1], Hidehiro Matsuoka[2], Seiya Kato[3], Masumi Kimoto[4] and Seiya Okuda[1]

[1]Division of Nephrology, [2]Cardiovascular Medicine, Department of Medicine, Kurume University School of Medicine, Kurume, [3]Division of Pathology and Cell Biology, Graduate School and Faculty of Medicine, University of Ryukyus, Okinawa and [4]Department of Nutritional Science, Faculty of Health and Welfare Science, Okayama Prefectural University, Soja, Japan

Abstract

Background. Decreased peritubular capillary (PTC) flow due to impaired endothelial function elicits tubulointerstitial ischaemia, thereby enhancing renal damage in chronic kidney disease, including diabetic nephropathy. Since nitric oxide (NO) is a vasodilator and known to play an important role in the maintenance of PTC flow, it is conceivable that asymmetric dimethylarginine (ADMA), an endogenous inhibitor of NO synthase, may cause tubulointerstitial ischaemia, thus being involved in the progression of diabetic nephropathy. In this study, we investigated whether overexpression of dimethylarginine dimethylaminohydrolase (DDAH), an enzyme that degrades ADMA, could improve tubulointerstitial ischaemia in streptozotocin (STZ)-induced diabetic rats.

Methods. Recombinant adenovirus vector encoding DDAH-I (Adv-DDAH) or control vector expressing bacterial β-galactosidase (Adv-LZ) was intravenously administrated to diabetic rats. Three days after the treatment, effects of DDAH overexpression on plasma or urinary levels of ADMA or NO metabolites (NOx), tubulointerstitial ischaemia and renal expression of transforming growth factor-β (TGF-β) were evaluated.

Results. Renal DDAH expression and activity were reduced in diabetic rats. Urinary levels of ADMA and TGF-β were increased, while NOx levels were decreased in diabetic rats. Compared with control rats, pimonidazole-detected hypoxic areas were larger in the kidney of diabetic rats, although the number of capillaries in tubulointerstitial regions was not different between the two groups. In addition, renal expression levels of hypoxia-inducible factor-1α (HIF-1α) and TGF-β were also increased in diabetic rats. DDAH overexpression significantly inhibited the increase of ADMA and the decrease of NOx and subsequently decreased urinary albumin excretion levels and ameliorated tubulointerstitial hypoxia and HIF-1α as well as TGF-β expression in diabetic rats.

Conclusion. The present study demonstrated for the first time that the suppression of ADMA by DDAH overexpression could improve tubulointerstitial ischaemia and subsequent renal damage in experimental diabetic nephropathy. Substitution of DDAH protein or enhancement of its activity may become a novel therapeutic strategy for the treatment of early diabetic nephropathy.

Keywords: asymmetric dimethylarginine; diabetic nephropathy; dimethylarginine dimethylaminohydrolase; endothelium; ischaemia

Introduction

Diabetic nephropathy (DN) is a leading cause of end-stage renal failure, which could account for disabilities and high mortality rates in patients with diabetes [1]. DN is characterized by functional and structural changes in the glomerulus, such as glomerular hyperfiltration, thickening of glomerular basement membranes and an expansion of extracellular matrix in mesangial areas [1]. However, it has recently been recognized that proximal tubular cell atrophy and tubulointerstitial fibrosis are more important than glomerulosclerosis in terms of renal prognosis [2,3]. Furthermore, accumulating evidence suggests that chronic renal hypoxia may have an important role in the progression of tubulointerstitial fibrosis in chronic kidney disease (CKD) including DN [2–4]. Chronic renal hypoxia could be elicited by several factors such as loss of peritubular capillaries (PTCs), decreased PTC flow, decreased nitric oxide (NO) production and/or bioavailability and activation of the renin–angiotensin system [2,3]. Indeed, Kang *et al.* recently demonstrated that the inhibition of NO synthase (NOS) accelerated renal damage in a remnant kidney model by eliciting PTC loss [5,6]. Since NO is not only a vasodilator but also a mediator of angiogenic signal [7], it is conceivable that decreased NO production and/or bioavailability may be linked to PTC loss and/or impaired PTC flow, which could contribute to tubulointerstitial ischaemia and fibrosis in DN.

Increased levels of asymmetric dimethylarginine (ADMA), an endogenous inhibitor of NOS, are associated with endothelial dysfunction in diabetes, which could

Correspondence and offprint requests to: Seiji Ueda, Division of Nephrology, Department of Medicine, Kurume University School of Medicine, 67 Asahi-machi, Kurume 830-0011, Japan. Tel: +81-942-31-7763; Fax: +81-942-31-7002; E-mail: ueda@med.kurume-u.ac.jp

account for accelerated atherosclerosis in this population [8–13]. Further, recently, we have shown that the reduction of ADMA by overexpression of dimethylarginine dimethylaminohydrolase (DDAH), a rate-limiting enzyme that mainly degrades ADMA, inhibits the progressive loss of PTCs in remnant kidney model rats, thereby protecting against renal damage in a rat model of CKD [14]. These observations led us to speculate that increased ADMA level may be a causative factor of PTC loss or impaired PTC flow, which could cause tubulointerstitial ischaemia and fibrosis in DN. Therefore, in this study, we investigated whether overexpression of DDAH could improve tubulointerstitial ischaemia and damage via decreased ADMA levels in streptozotocin (STZ)-induced diabetic rats.

Methods

Animal preparation

Seven-week-old male Sprague-Dawley rats received 60 mg/kg intraperitoneal injection of STZ in a 10 mmol/L citrate buffer. Control non-diabetic rats (control: $n = 10$) received a citrate buffer alone. Animals with blood glucose levels >350 mg/dL 48 h later were considered to be diabetic. Fourteen days after the injection, rats were divided into two groups: diabetic rats treated with tail vein injection of 1.5×10^{10} plaque-forming units of control vector expressing bacterial β-galactosidase (Adv-LZ) (STZ + Adv-LZ: $n = 10$) and those with that of recombinant adenovirus vector encoding DDAH-I (Adv-DDAH) (STZ + Adv-DDAH: $n = 10$) [14–16]. Three days after adenovirus infection, the rats were killed. As shown in the previous publications [14,15], we confirmed that adenoviral DDAH infection actually increased its expression in liver and kidney (Figure 1A).

Chemical analysis

Urinary albumin excretion (UAE) levels were determined with commercially available ELISA kits (Exocell, Philadelphia, PA, USA). Plasma and urinary levels of NO metabolites (NOx: nitrate plus nitrite), L-arginine, ADMA and symmetric dimethylarginine (SDMA) were measured by a high-performance liquid chromatography as described previously [14–16].

Measurement of enzymatic activity of DDAH

Total DDAH activity was measured as described previously [14–16]. Briefly, homogenized kidney tissues were incubated with 4 μmol/L ADMA and 0.1 mol/L sodium phosphate buffers (pH 6.5) in a total volume of 0.5 mL for 6 h at 37°C. The reaction was stopped by the addition of an equal volume of 10% trichloroacetic acid, and the supernatant was boiled with diacetyl monoxime [0.8% (wt/vol) in 5% acetic acid] and antipyrine [0.5% (wt/vol) in 50% sulfuric acid]. The amounts of L-citrulline formed were determined with the spectrophotometric analysis at 466 nm.

Immunohistochemistry

The kidneys were removed and fixed in 4% paraformaldehyde. Then the kidneys were embedded in paraffin wax for sectioning. Three-micrometre paraffin sections were incubated with a monoclonal JG-12 antibody raised against aminopeptidase P of capillary endothelial cells (ECs) (Bender MedSystems, San Bruno, CA, USA). After exposure to the peroxidase-labelled secondary anti-mouse antibody, the sections were incubated with the 3,3′-diaminobenzidine solution. Hypoxic area was detected by using pimonidazole (Chemicon) staining as previously described [3,4,17]. The intensity of JG-12 or pimonidazole staining was quantitatively analysed by image analysis software (Optimas version 6.57; Media Cybernetics, Silver Spring, MD, USA).

Western blot analysis

The kidney cortex tissues were homogenized and lysed with 25 mmol/L Tris–HCl (pH 7.4) containing 1% Triton X-100, 0.1% SDS, 2 mmol/L EDTA and 1% protease inhibitor cocktail (Nakarai Tesque, Kyoto, Japan). Then the supernatant was separated by SDS–PAGE and transferred to nitrocellulose membranes (Biorad, Hercules, CA, USA) as described previously [18]. Immune complexes were visualized with an enhanced chemiluminescence detection system (ECL; Amersham Bioscience, Buckinghamshire, UK). A monoclonal antibody against hypoxia-inducible factor-1α (HIF-1α) was purchased from Novus Biologicals (Littleton, CO, USA), and a polyclonal antibody directed against endothelial NOS (eNOS) was from Santa Cruz Biotechnology (Santa Cruz, CA, USA).

Semi-quantitative reverse transcription-polymerase chain reactions (RT-PCR)

Poly(A)$^+$RNAs were isolated from the kidney and then analysed by RT-PCR as described previously [14,15]. Forward and reverse primer sequences were 5′-CGTGGCCGTGGTGTGCGAGGA-3′ and 5′-CAGTTCAGACATGCTCACGGGG-3′ for detecting DDAH-I, 5′-AGAATTGTGGAGATGGGGGATGAG-3′ and 5′-CAACCCAGGACGCAGAAAGAGAC-3′ for detecting DDAH-II, 5′-AACTGAAGCTCGCACTCTCG-3′ and 5′-TCAGCACAGATCTCCTTGGC-3′ for detecting PRMT-1, 5′-AGACATTCGGGAAGCAGTGCCAG-3′ and 5′-CATGAGGAGCAGGAAGGGTCGG-3′ for detecting transforming growth factor-β (TGF-β) and 5′-AGACAGCCGCATCTTCTTGT-3′ and 5′-CCACAGTCTTCTGAGTGGCA-3′ for detecting GAPDH mRNAs.

Measurement of urinary levels of TGF-β

TGF-β1 in the urine was measured using a sandwich enzyme-linked immunosorbent assay (ELISA) kit (Quantikine, R&D Systems, Minneapolis, MN, USA) as described previously [19]. Values were expressed as urinary levels of TGF-β/creatinine (pg/mg).

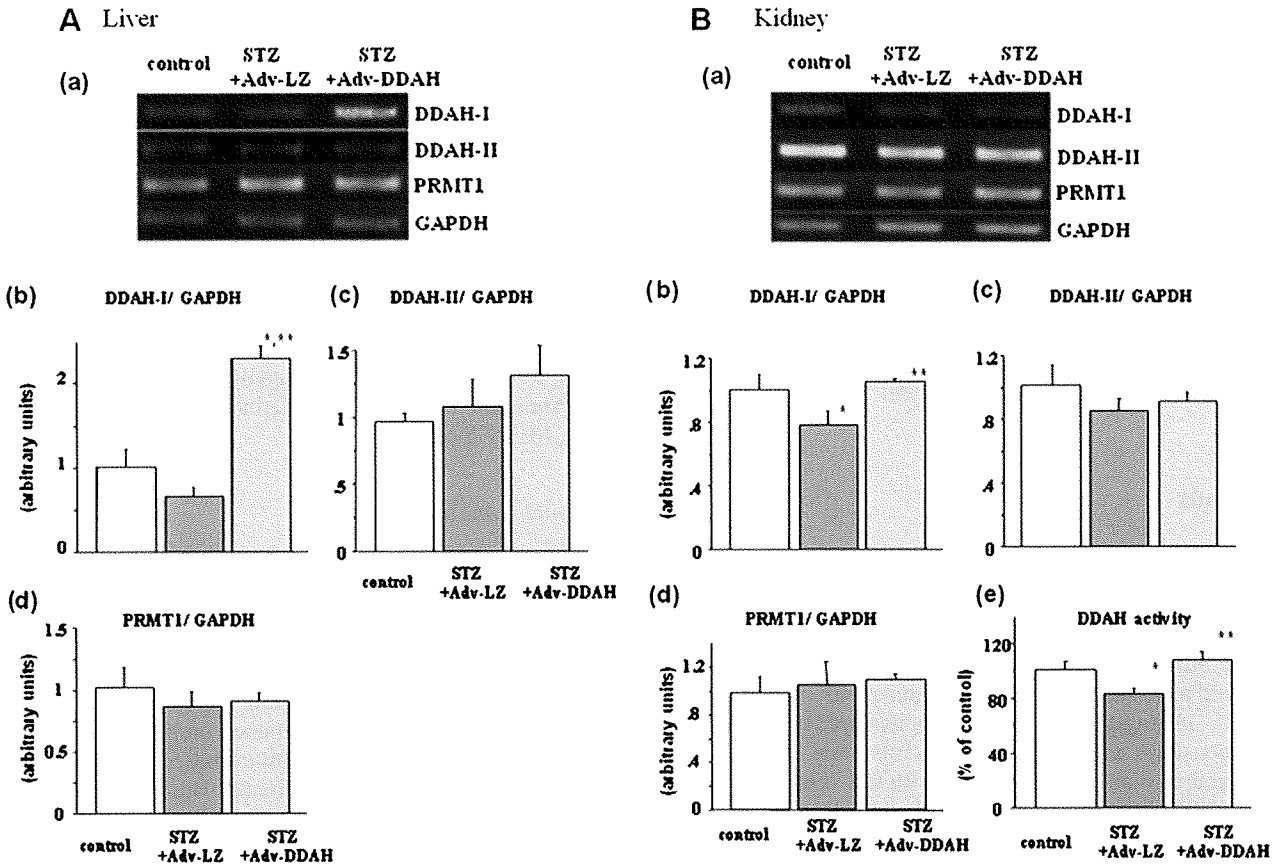

Fig. 1. Effects of diabetes or DDAH-I overexpression on DDAH-I, DDAH-II and PRMT1 expression in liver (**A**) and kidney (**B**). Upper panels (**a**) show the representative results of RT-PCR. Lower panels show the quantitative data of DDAH-I (**b**), DDAH-II (**c**) and PRMT1 (**d**) gene expression. Data were normalized by the intensity of GAPDH mRNA-derived signals and related to the value of the control. (**e**) Renal enzymatic activity of DDAH. $^{*}P < 0.05$ compared to the value of the control. $^{**}P < 0.05$ compared to the value of the STZ-Adv-LZ.

Statistical analyses

All data are presented as means ± SE. Analysis of variance (ANOVA) was performed for all studied parameters with Scheffe's *post hoc* test to compare variables among experimental groups. A P-value <0.05 was considered statistically significant.

Results

Clinical parameters of animals

As shown in Table 1, compared with the control, plasma glucose levels were elevated and body weights were significantly lower in STZ+Adv-LZ. Overexpression of DDAH did not affect glucose levels or body weight in diabetic rats. There were no significant differences of systolic blood pressure, heart rate or serum creatinine levels among the three groups. Creatinine clearance and urinary albumin excretion (UAE) levels were increased in diabetic rats (Table 1). DDAH overexpression significantly reduced UAE levels, but not creatinine clearance. Further, as shown in Figure 1B, renal DDAH-I gene expression and activity were decreased in diabetic rats, which were restored with the treatment of the adenoviral DDAH-I gene transfer. Renal and liver gene expressions of DDAH-II and protein arginine methyltransferases 1 (PRMT1), an important enzyme for ADMA synthesis, were not different among the three groups (Figure 1).

Plasma ADMA levels tended to increase in STZ+Adv-LZ, which was significantly reduced by DDAH infection (Figure 2A). Compared with non-diabetic control, urinary excretion levels of ADMA were increased and NOx levels were decreased in STZ + Adv-LZ, both of which were suppressed by DDAH overexpression (Figures 2C and 1F). There were no significant differences in plasma or urinary levels of SDMA, an inert isomer of ADMA, which is not degraded by DDAH (Figure 2B and D), among the groups. Further, plasma L-arginine levels were significantly lower in STZ+Adv-LZ, which were not affected by the treatment with DDAH infection (Figure 2E).

Measurement of the number of renal capillaries

We first examined the effects of diabetes or DDAH overexpression on PTC loss in our models. For this, renal capillary ECs were stained with a JG-12 antibody directed against

Table 1. Clinical parameters

	Control ($n = 10$)	STZ + Adv-LZ ($n = 10$)	STZ + Adv-DDAH ($n = 10$)
Plasma glucose (mg/dL)	152 ± 10	512 ± 23*	476 ± 34*
Body weight (g)	370 ± 6	285 ± 7*	286 ± 8*
Systolic blood pressure (mmHg)	106 ± 3	110 ± 3	113 ± 2
Heart rate (bpm)	351 ± 8	302 ± 20	338 ± 21
Serum creatinine (mg/dL)	0.24 ± 0.01	0.24 ± 0.01	0.27 ± 0.02
Creatinine clearance (mL/min)	3.4 ± 0.08	4.2 ± 0.45*	3.7 ± 0.56
Urinary albumin excretion (mg/g creatinine)	28.0 ± 6.1	263 ± 56*	101 ± 35**

*$P < 0.05$ compared with the value of the control.
**$P < 0.05$ compared with the value of the Adv-LZ-treated diabetic rats.

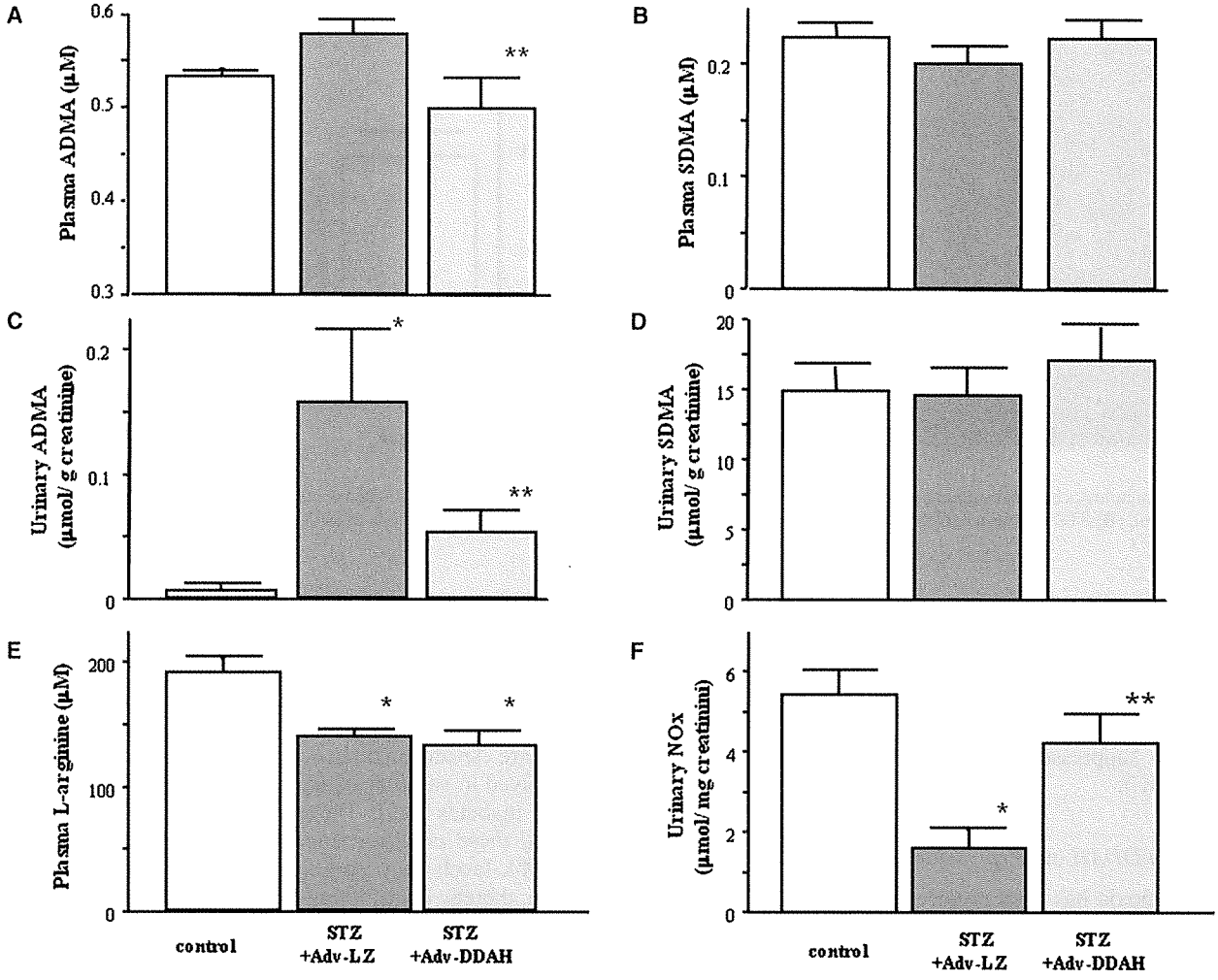

Fig. 2. Plasma and urinary levels of methylated arginine, L-arginine and NOx. Plasma levels of ADMA (**A**), SDMA (**B**) and L-arginine (**E**) and urinary levels of ADMA (**C**), SDMA (**D**) and NOx (**E**) were measured by an HPLC. *$P < 0.05$ compared to the value of the control. **$P < 0.05$ compared to the value of the STZ+Adv-LZ.

aminopeptidase P, a specific marker for ECs [14]. As shown in Figure 3, there were no significant differences in the number of renal capillaries in tubulointerstitial or glomerular regions among the three groups. We also confirmed that expression levels of endothelial NOS, another marker for ECs, were not different among the groups by western blot analysis (data not shown).

Effects of DDAH overexpression on tubulointerstitial ischaemia

We next investigated the effects of diabetes or DDAH overexpression on tubulointerstitial ischaemia in our models. For this, we immunostained hypoxic areas by using pimonidazole, a hypoxic probe [3,4,17]. As shown in

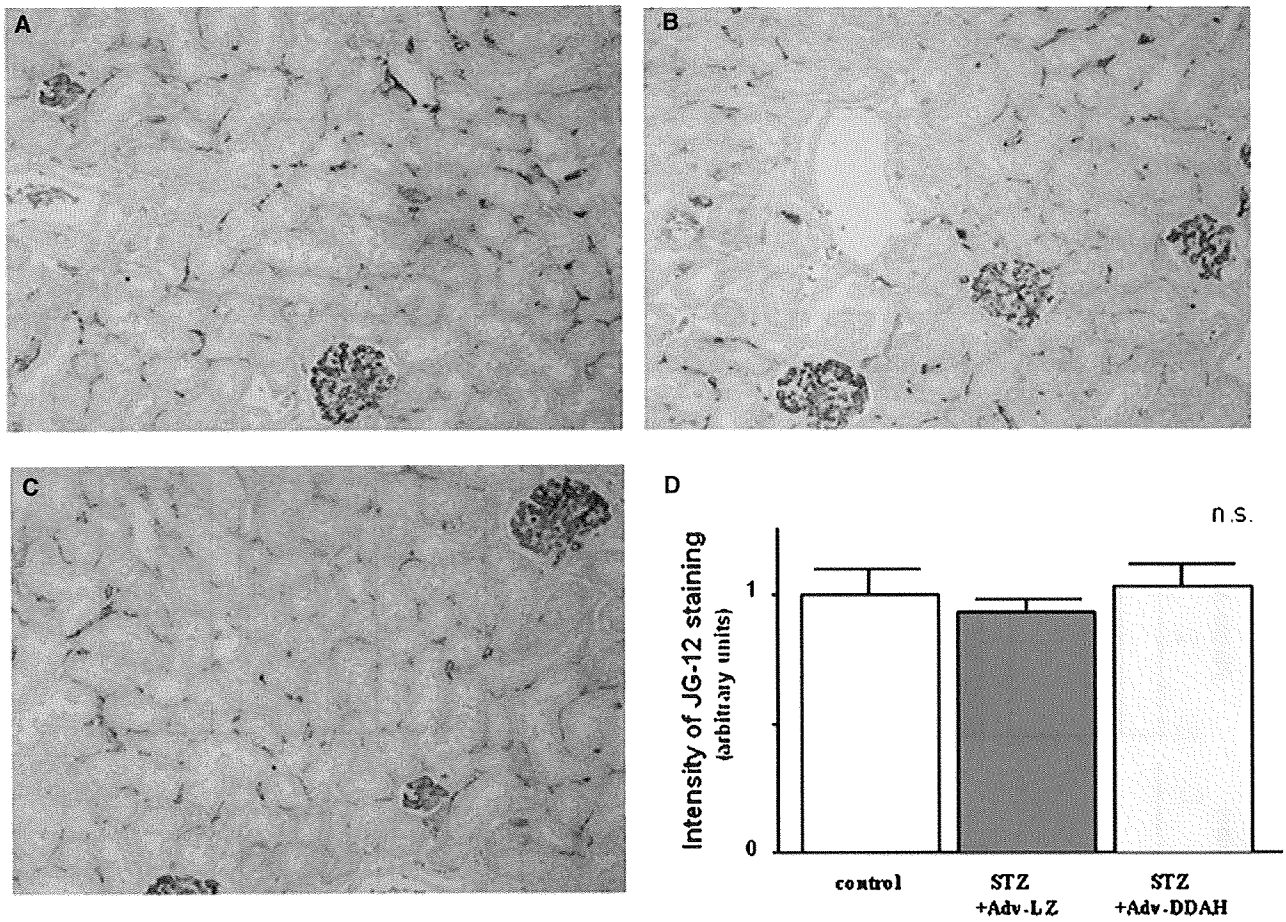

Fig. 3. Immunohistochemical staining of renal capillaries. Renal capillary ECs were stained with the JG-12 antibody directed against aminopeptidase P. (**A**) control, (**B**) STZ + Adv-LZ, (**C**) STZ+Adv-DDAH. Magnification ×200. (**D**) Quantitative analysis of PTC staining. n.s.: not significant.

Figure 4A and B, intensity of pimonidazole staining was increased in tubulointerstitial areas of the kidney cortex of STZ+Adv-LZ, which was significantly blocked by DDAH overexpression. Further, renal expression of HIF-1α protein was up-regulated in STZ+Adv-LZ, which was also suppressed by the treatment with Adv-DDAH (Figure 4C).

Effects of DDAH overexpression on TGF-β expression

Since hypoxia has been reported to stimulate TGF-β synthesis in tubular cells [12,20], we further studied the effects of DDAH overexpression on TGF-β expression in the kidney. As shown in Figure 5A, semi-quantitative RT-PCR revealed that DDAH overexpression inhibited up-regulation of renal TGF-β gene expression in STZ+Adv-LZ. Urinary excretion levels of TGF-β were increased in STZ+Adv-LZ, which were also blocked by the treatment with Adv-DDAH (Figure 5B).

Discussion

The salient finding of this study was that overexpression of DDAH, a rate-limiting enzyme that mainly degrades ADMA, not only decreased plasma and urinary excretion levels of ADMA, but also improved the increase in UAE and tubulointerstitial ischaemia and subsequently suppressed TGF-β up-regulation in the early phase of experimental DN.

There are several papers to show that plasma levels of ADMA are elevated in diabetic animals or patients, thus being involved in vascular injury and accelerated atherosclerosis in diabetes [8,9]. Therefore, the present study has extended these previous findings showing that elevation of ADMA levels may participate in tubulointerstitial ischaemia, thereby contributing to the development and progression of DN. In this study, renal DDAH-I expression and activity were decreased in diabetic rats, which were ameliorated by the treatment of the adenoviral DDAH-I gene transfer. Further, overexpression of DDAH not only lowered urinary levels of ADMA, as well as increased the reduced levels of urinary NOx generation, but also improved tubulointerstitial ischaemia in STZ+Adv-LZ. These observations suggest that the decreased metabolism of ADMA by DDAH may be mainly involved in tubulointerstitial ischaemia in DN. In support of this speculation, decreased enzymatic activity or expression of DDAH has been reported in STZ-induced diabetic rats, which could be correlated with the elevation of ADMA in this animal [8,21]. In the present study, we found that urinary excretion levels of

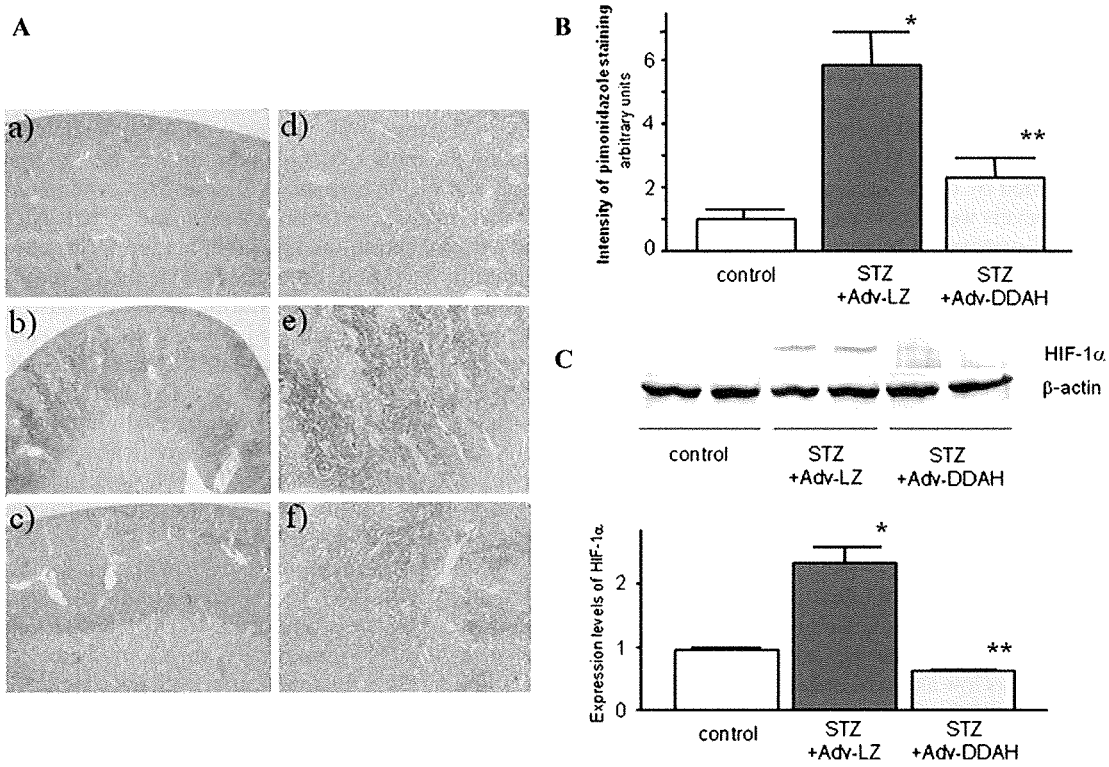

Fig. 4. Tubulointerstitial ischaemia. (**A**) Immunohistochemical staining of hypoxic area with pimonidazole. (**a**) and (**d**) Control; (**b**) and (**e**) STZ+Adv-LZ; (**c**) and (**f**) STZ+Adv-DDAH. (**a**)–(**c**) Magnification ×12.5; (**d**)–(**f**) magnification ×40. (**B**) Quantitative analysis of pimonidazole staining. $^{*}P < 0.01$ compared to the value of the control. $^{**}P < 0.01$ compared to the value of STZ-Adv-LZ. (**C**) Western blot analysis for HIF-1α. The upper panel shows the representative results of western blotting. The lower panel shows the quantitative data. Data were normalized by the intensity of β-actin and related to the value of the control ($n = 10$, each). $^{*}P < 0.05$ compared to the value of the control. $^{**}P < 0.05$ compared to the value of the STZ-Adv-LZ.

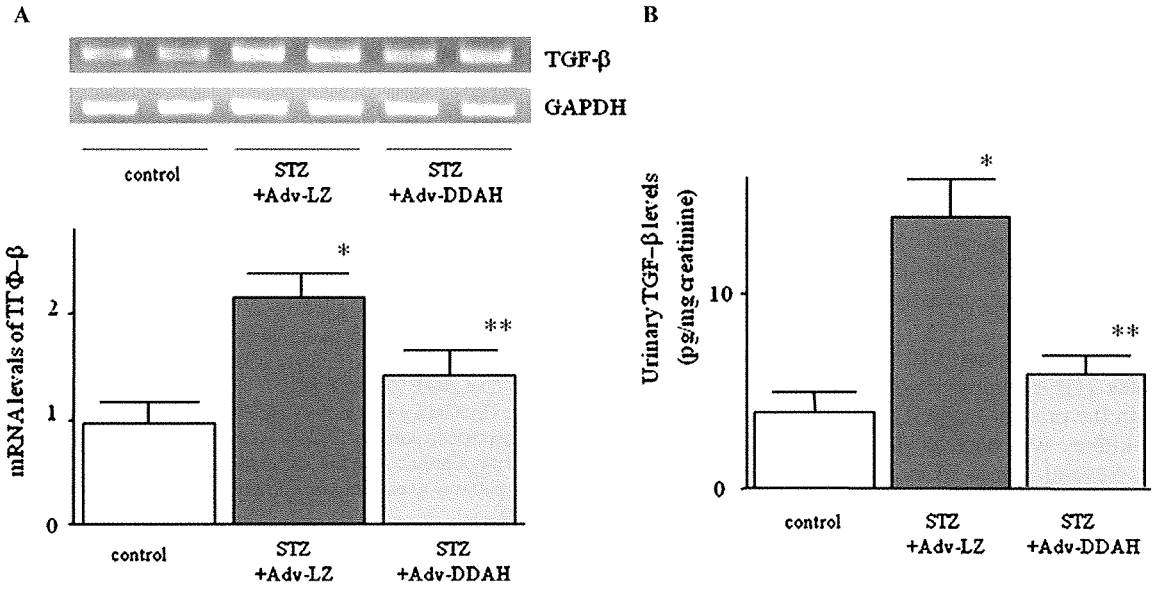

Fig. 5. Effects of DDAH overexpression on TGF-β expression. (**A**) The upper panel shows the representative results of RT-PCR. The lower panel shows the quantitative representation of TGF-β gene induction. Data were normalized by the intensity of GAPDH mRNA-derived signals and related to the value of the control ($n = 10$, each). (**B**) Urinary levels TGF-β ($n = 10$, each). $^{*}P < 0.05$ compared to the value of the control. $^{**}P < 0.05$ compared to the value of the STZ-Adv-LZ.

SDMA, a structural isomer of ADMA, were not changed among the three groups (Figure 2D). Since cellular uptake of SDMA is mediated by a y+ transporter, which is also known to be involved in ADMA uptake [22,23], it is unlikely that decreased tubular uptake could play a role in increased urinary excretion of ADMA.

As previously reported by other researchers [24,25], we found that L-arginine levels were decreased in diabetic rats. In this study, reduced urinary NOx generation and tubulointerstitial ischaemia were ameliorated by the treatment of Adv-DDAH, although DDAH infection did not affect the L-arginine levels in STZ+Adv-LZ. Further, it has been reported that L-arginine concentration as low as 3 μM is sufficient to induce half-maximal activity of NOS *in vitro* [26,27]. These observations suggest that it is unlikely that reduced L-arginine levels could contribute to the decrease in urinary NOx generation and tubulointerstitial ischaemia in our models. However, we cannot totally exclude the possibility that L-arginine could play a role in our systems because there are numerous studies that L-arginine supplementation could augment NO production in humans and thereby improve endothelium-dependent vasodilatation [28]. *In vivo*, specifically, in the presence of ADMA, L-arginine concentration as low as 3 μM may 'NOT' be sufficient to induce half-maximal activity of endothelial NOS, and therefore the L-arginine/ADMA ratio could be a good marker for NO generation [28,29].

NO is not only a vasodilator but also a mediator of the angiogenic signal [7]. Therefore, it is conceivable that elevation of ADMA could cause PTC loss and/or impaired PTC flow by reducing renal production of NO, which may in concert contribute to tubulointerstitial ischaemia and fibrosis in DN. In this study, diabetes or DDAH overexpression did not affect PTC loss (Figure 3). Therefore, decreased metabolism of ADMA by DDAH may cause tubulointerstitial ischaemia via impaired PTC flow in our models.

In the present study, UAE levels were increased in diabetic rats, which were blocked by the treatment of DDAH infection (Table 1). Caglar *et al.* previously reported that ADMA levels were correlated with proteinuria in patients with CKD stage I [30]. Since there is a growing body of evidence that endothelial dysfunction is linked to proteinuria [31–33], the present observations suggest that DDAH could ameliorate endothelial dysfunction and subsequently reduce UAE levels in diabetic rats via suppression of ADMA.

We have previously shown that DDAH overexpression down-regulates TGF-β expression in a rat remnant kidney model [14]. In the present study, TGF-β overexpression in the diabetic kidney was decreased by the treatment with Adv-DDAH. Several pieces of evidence have implicated the TGF-β as a major etiologic agent in the pathogenesis of tubulointerstitial fibrosis in DN [34,35]. Furthermore, there are several papers to show that the TGF-β gene is up-regulated under hypoxic conditions [20]. These observations suggest that the ADMA-mediated tubulointerstitial ischaemia may be involved in TGF-β induction and tubulointerstitial fibrosis in DN. In addition, exogenous administration of ADMA to humans caused a long-lasting decrease in renal perfusion even at doses that failed to alter blood pressure [36], thus further supporting the concept that ADMA could elicit tubulointerstitial ischaemia in the early phase of DN.

A number of studies about the effects of high glucose and/or diabetes on the renal NO system have often produced contradictory findings [37]. The use of different techniques for estimating the renal NO concentration and activity may explain some of the discrepancies. However, Keynan *et al.* reported that urinary NO production and renal NOS levels and activity determined by combination techniques, including immunoblotting, immunohistochemistry and diaphorase staining, were reduced during the early phase of experimental diabetes mellitus [38]. In addition, Palm *et al.* have recently shown that the reduced bioavailable NO concentration in the renal cortex directly measured by microsensors is associated with the decreased renal blood perfusion in the early phase of STZ-induced diabetes [25]. These findings support our concept that ADMA could contribute to early DN by causing tubulointerstitial ischaemia via suppression of renal NO generation.

In conclusion, the present observations suggest the active participation of ADMA–DDAH axis in tubulointerstitial ischaemia in DN. Recently, it has been reported that plasma levels of ADMA could be a strong predictor for the progression of renal dysfunction in patients with CKD [39,40], further supporting the clinical relevance of ADMA in chronic ischaemia and progression of renal injury. Substitution of DDAH protein or enhancement of its activity may become a novel therapeutic strategy for the treatment of DN. To show the direct evidence for the cause–effect relationship between NO bioavailability and tubulointerstitial ischaemia, whether NOS inhibition by L-NMMA could cause similar renal tubular damage in diabetic rats and if L-arginine could restore such damages should be clarified.

Acknowledgements. We thank Ms M. Miura, Ms A. Yamaguchi and Ms F. Imamura for excellent technical support. This work was supported in part by grants from Grant-in-Aid for Scientific Research from the Ministry of Education, Science and Culture, Tokyo, and from Japan Foundation of Cardiovascular Research, Tokyo.

Conflict of interest statement. None declared.

References

1. Ziyadeh FN, Hoffman BB, Han DC *et al.* Long-term prevention of renal insufficiency, excess matrix gene expression, and glomerular mesangial matrix expansion by treatment with monoclonal antitransforming growth factor-beta antibody in db/db diabetic mice. *Proc Natl Acad Sci USA* 2000; 97: 8015–8020
2. Fine LG, Orphanides C, Norman JT. Progressive renal disease: the chronic hypoxia hypothesis. *Kidney Int* 1998; 65(Suppl): S74–S78
3. Nangaku M. Chronic hypoxia and tubulointerstitial injury: a final common pathway to end-stage renal failure. *J Am Soc Nephrol* 2006; 17: 17–25
4. Rosenberger C, Khamaisi M, Abassi Z *et al.* Adaptation to hypoxia in the diabetic rat kidney. *Kidney Int* 2008; 73: 34–42
5. Kang DH, Nakagawa T, Feng L *et al.* Nitric oxide modulates vascular disease in the remnant kidney model. *Am J Pathol* 2002; 161: 239–248
6. Kang DH, Joly AH, Oh SW *et al.* Impaired angiogenesis in the remnant kidney model: I. Potential role of vascular endothelial growth factor and thrombospondin-1. *J Am Soc Nephrol* 2001; 12: 1434–1447
7. Murohara T, Asahara T, Silver M *et al.* Nitric oxide synthase modulates angiogenesis in response to tissue ischemia. *J Clin Invest* 1998; 101: 2567–2578